5-2022

Coastal Sediment Response to the Diel Oxygen Cycle

Kara Gadeken
University of South Alabama, kgadeken@disl.org

COASTAL SEDIMENT RESPONSE TO THE DIEL OXYGEN CYCLE

A Dissertation

Submitted to the Graduate Faculty of the
University of South Alabama
in partial fulfillment of the
requirements for the degree of

Doctor of Philosophy

in

Marine Sciences

By
Kara J. Gadeken
B.S., College of William & Mary, 2014
May 2022

ACKNOWLEDGEMENTS

Thank you to everyone who has helped me throughout this process. Firstly to my advisor Kelly Dorgan - I couldn't have asked for a more wonderful graduate advisor. I am a better scientist and a better person for having worked with you. Second, to my committee members; John, Sinéad, Behzad and Sarah, for their guidance and patience with my wandering path down the road towards my degree. Thank you to the organizations and funding sources that supported this work, including the University of South Alabama Center for Environmental Resiliency (CER) Grant 279806-421200-4200, NSF OCE CAREER Grant 1844910 and ONR Award N00014-18-1-2806 to KMD, and Southern Association of Marine Laboratories Student Support Program. Also to the students, faculty and staff at the Dauphin Island Sea Lab and the University of South Alabama who have assisted me along the way. Thank you to past and present members of the Dorgan Lab, particularly W.C. Clemo, W. Ballentine, E. Kiskaddon, C. Cox, and M. Frey. I hope every lab I'm a part of will be as collaborative and fun. Special thanks to G. Lockridge for the countless patient hours spent helping me in the workshop, and B. Dzwonkowski for his advice and good humor. And lastly, heartfelt thanks to my friends and family for their love, encouragement, and support over the years.

TABLE OF CONTENTS

Page

LIST OF TABLES

LIST OF FIGURES

Appendix Figures

LIST OF ABBREVIATIONS

DO……Dissolved Oxygen

OM……Organic Matter

OMM……Oxygen Manipulation Machine

pCO_2……partial pressure of Carbon Dioxide

RSS……Residual Sum of Squares

SOD……Sediment Oxygen Demand

ABSTRACT

Kara J. Gadeken, PhD, University of South Alabama, May 2022. Coastal Sediment Response to the Diel Oxygen Cycle. Chair of Committee: Kelly M. Dorgan, PhD.

Shallow coastal sediments are sites of intense respiration and organic matter breakdown. Macroinfauna bioturbate and bioirrigate sediments which supplies microbes with oxygen and newly deposited organic material from surface sediments, facilitating microbial remineralization of organic matter. These processes depend heavily on the concentration of dissolved oxygen in overlying water. Shallow water oxygen patterns often follow a diel cycle as dissolved oxygen decreases at night due to respiration and then increases during the day with photosynthesis, creating recurring suboxic conditions that are potentially stressful to organisms. Sediment oxygen flux is known to depend on ambient dissolved oxygen concentration, but behavioral responses of macrofauna to low oxygen can be complex and diverse, introducing variability into sediment metabolism rates.

This dissertation research examined the effects of diel changes in dissolved oxygen on macrofaunal behavior and activities and corresponding changes in sediment metabolism throughout the diel cycle. I constructed a simple laboratory system to manipulate dissolved oxygen concentrations into a diel pattern and exposed sediment infauna to repeated diel oxygen cycles. Sediment mixing in all three of the tested taxa decreased overall throughout the experiment and over two diel cycles, but also varied proportionally with oxygen within each diel exposure. Behaviors did not show significant variation with the diel cycle, though this is likely because behaviors relevant to sediment

mixing activity were not easily detected or quantified with the employed methods. These results indicate that experiments quantifying sediment mixing by macrofauna that occur in fully oxygenated conditions may not be representative of in situ rates, and that it may require more even than a single diel cycle for representative rates to emerge.

To better understand how natural macrofaunal assemblages affect sediment metabolism when exposed to diel cycling oxygen, I conducted a field sediment metabolism experiment. Flow-through sediment metabolism chambers were constructed and deployed to measure in situ sediment oxygen consumption. The presence of macrofauna drove overall greater and more variable rates sediment oxygen demand particularly at night, presumably due to fauna responding to low oxygen by increasing their irrigation activity. This research shows that in coastal sediments, variation on small temporal and spatial scales interact to affect sediment metabolism.

Sediment metabolism, a key ecosystem function, is controlled by complex networks of interactions and feedbacks between biogeochemical and ecological processes. This research sheds new light on the connection between oxygen concentration and oxygen consumption in these dynamic, productive marine systems and improves our understanding of the role of macrofauna in modulating that relationship.

CHAPTER I A SIMPLE AND INEXPENSIVE METHOD TO MANIPULATE DISSOLVED OXYGEN IN THE LAB

The contents of this chapter were previously published as an open access journal article (doi: 10.5670/oceanog.2021.202) in the journal *DIY Oceanography* and made publicly available under the terms of the Creative Commons Attribution 4.0 International License which allows the use, sharing, adaptation, distribution, and reproduction in any medium or format providing appropriate citation (Gadeken and Dorgan 2021). There have been no changes made to the content of this article from the published version.

1.1 Purpose of Device

Changes in dissolved oxygen concentration can cause dramatic shifts in chemical, biological and ecological processes in aquatic systems. In shallow coastal areas, this can happen on short time scales, with oxygen increasing during the day due to photosynthesis and declining at night due to respiration. We present a system controlled by an Arduino microprocessor which leverages the oxygen-consuming capacity of sediments to manipulate dissolved oxygen in an aquarium tank to planned concentrations. With minor adjustments to the Arduino code, the system can produce a variety of dissolved oxygen patterns, including a diel cycle. The system is designed to be user-friendly and scalable if needed, using easily acquired and low-cost electronic and aquarium components. The simplicity and accessibility of this system allows for deeper exploration of the effects of dissolved oxygen variability in aquatic systems, and the use of Arduino code and basic electronics make it a potential tool to teach experimental design and instrument fabrication.

1.2 Background

The availability of dissolved oxygen (DO) is a major factor governing aquatic ecosystem function and is an indicator of water quality and ecosystem health (Diaz and

Rosenberg 1995, 2011; Wenner et al. 2004; Middelburg and Levin 2009). The concentration of DO in aquatic environments is controlled by the balance of oxygen sources (mixing with the atmosphere, advection of oxygenated water, photosynthetic production) and sinks (aerobic respiration and abiotic oxidation), and shifts in this balance result in cascading chemical, biological and ecological effects (Middelburg and Levin 2009). Changes in DO concentration occur across temporal and spatial scales, from widespread seasons-long bottom hypoxia on continental margins to dramatic daily or sometimes hourly oxygen fluctuations in shallow, semi-enclosed coastal lagoons or embayments. Most low oxygen events are this second type, relatively short in duration but occurring frequently (Wenner et al. 2004). Although many researchers have examined the effects of declining or persistent low DO on water and sediment chemistry (McCarthy et al. 2008; Lehrter et al. 2012; Neubacher et al. 2013; Foster and Fulweiler 2019) and organismal behavior and physiology (Diaz and Rosenberg 1995; Long et al. 2008; Levin et al. 2009; Sturdivant et al. 2012; Riedel et al. 2014; Calder-Potts et al. 2015), it is far less common to see investigations into dynamic variation in DO, likely because of the difficulties in precisely and repeatedly manipulating DO in the lab.

DO can easily be increased in water by bubbling with air but decreasing DO requires either chemical consumption or physical expulsion of oxygen from solution. An often-used method of decreasing DO involves stripping it from the water by bubbling with N_2 gas. Studies of low oxygen effects that run for multiple weeks or months, however, may require large amounts of N_2 gas which can be expensive, prompting investigations into ways to reduce the amount of gas needed (Bevan and Kramer 1988; Peterson and Ardahl 1992; Grecay and Stierhoff 2002). Oxygen can also be removed by

"vacuum degassing", applying a partial vacuum to the water to remove DO from solution. This requires an airtight vacuum setup that may not be feasible for some researchers (Mount 1961; Miller et al. 1994). More recently, researchers have developed methods that rely on chemical consumption rather than physical removal of DO to produce low oxygen water. Thetmeyer et al. (1999) leveraged the respiration of the fish study subject itself to draw down DO, controlling hypoxic, normoxic, and oscillating oxygen treatments with an automated system (Thetmeyer et al. 1999). For this method to work the fish must consume enough oxygen to change the DO of the experimental environment, which may not be possible for smaller study subjects or those for which wall effects are a concern. Long et al. (2008) presented an alternative method using sediments to decrease DO by percolating water through a "fluidized mud reactor" that consumed oxygen (Long et al. 2008). The resulting anoxic water was then mixed in different proportions with fully oxygenated water to produce predetermined DO concentrations. This setup is convenient for creating water with stable DO concentrations but does not easily allow for complex manipulations of DO change through time.

The existing DO manipulation methods pose a barrier to entry for many researchers because of their cost and complexity. Additionally, many methods have been designed to simulate long-term hypoxia, whereas in coastal systems, DO concentrations can vary on short time scales. Here we describe and test a DO manipulation system that can be constructed in a laboratory or classroom setting using easily acquired electronic and aquarium components. The closed-loop system does not require N_2 gas purging or vacuum degassing; instead it relies on sediment oxygen demand (SOD) to draw DO down and increases DO by periodically opening a solenoid valve to allow oxygenated

water to flow in from an upstream reservoir tank (Figure 1). The provided code is uploaded to an Arduino microprocessor that monitors and adjusts the DO in the experimental tank to a pattern planned by the user, simultaneously recording and displaying the DO data. This system was built to study behavior and SOD by infaunal organisms held individually in small sediment-filled aquaria (Figure 1) but could be used for a variety of shallow-water systems and study organisms. This simple, low-cost and open-source method of manipulating DO in the lab will allow for more varied studies into how change in DO affects aquatic systems.

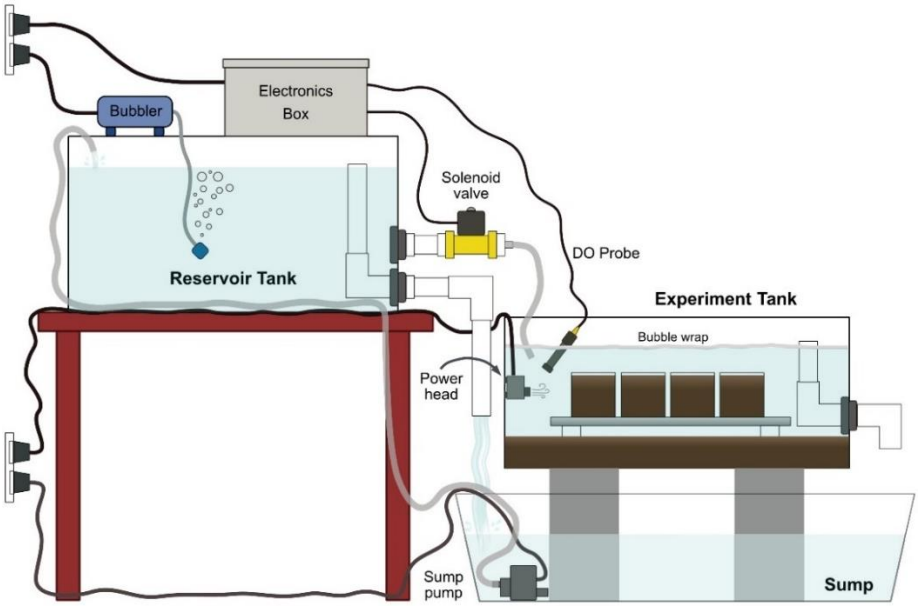

Figure 1. Diagram of oxygen manipulation setup. It is a closed-loop system, constantly cycling water between an oxygenated reservoir tank and a sump. When the dissolved oxygen (DO) in the experiment tank is sensed to be lower than the desired level due to sediment consumption, the solenoid valve is opened, allowing oxygenated water to flow in. A power head in the experiment tank ensures that the water is well mixed, and a layer of bubble wrap floating at the water surface prevents diffusion of atmospheric oxygen into the water. PVC pipe is shown in white, tubing in gray, and wiring in black. Note that, though only one experiment tank is depicted here, several replicate experiment tanks would be needed or several replicate trials should be performed to avoid pseudoreplication.

1.3 Materials and Costs

The components in the system are outlined in Table 1. We estimate the total cost of constructing this system to be approximately $625 in 2021, not including shipping expenses.

Table 1. Components list for laboratory dissolved oxygen experiments. Prices are in US dollars.

Electronics components	Price
AC to DC power converter	12
Dual row terminal strip block	10
Arduino Mega 2560 rev3	40
Adafruit Assembled Data Logging shield	15
SD card	9
3V coin cell battery	5
Atlas Scientific Dissolved Oxygen Kit	283
12V solenoid valve (normally closed)	20
12V relay	5
DC power pigtail cable	7
On/off toggle switch	4
5V I2C LCD display (Qunqi)	7
12V to 5V power converter	10
USB cable (arduino to PC)	6
Electrical wire, 10 KΩ resistor, push button	10
Electronics box	22

Aquarium components	Price
Reservoir tank	10
Aquarium bubbler, air tubing, air stones	10
Sump	10
Sump pump (Marineland MJ1200)	30
Flexible tubing	15
Experimental tank	30
Power head	20
Threaded bulkheads (x3)	10
PVC piping	15
PVC pipe connectors	10

Total	Price
	625

Note that the components list consists only of consumable items (e.g. wire, tubing, plumbing) and specialized equipment (e.g. Arduino, Atlas Scientific EZO DO kit, pumps, solenoid valve). Non-consumables and tools needed for assembly are not included because it is assumed that the user will already have access to many of these

items. Cost of construction might also be substantially lowered if materials can be purchased individually rather than in large packs, or scavenged from other projects, as only a single or very small amount is required for most components. A student at an undergraduate level or a particularly capable high school student should be able to construct and begin using the system within a couple of weeks.

1.4 Assembly Steps

First assemble the electronics according to the wiring diagram (Figure 2). The Arduino Mega®, solenoid and relay may all be powered by the same 12V power source. The Adafruit® data logging shield is mounted directly to the Arduino via soldered header pins, and the Atlas Scientific® EZO DO circuit is mounted on an electrically isolated EZO carrier board and connects to the SCL (clocking) and SDA (data-transmitting) pins on the data logging shield to communicate with the Arduino (Figure 2). Communication between the Arduino and the EZO DO circuit is in I^2C protocol to allow for easy addition of secondary devices, in case more circuits and sensors are desired to scale the system up. The EZO DO circuit must be converted to I^2C protocol and the I^2C address changed to correspond to the address defined in the oxygen manipulation code to communicate with the Arduino. The EZO DO circuit should also be adjusted with temperature and salinity offsets and two-point oxygen calibrated before each use. Directions on conversion to I^2C protocol, offset adjustments and calibration are in the EZO DO circuit documentation. An LCD screen is included to display the average measured DO over the previous several measurements and the planned DO, allowing the user to easily assess whether the system is functioning properly and following the prescribed pattern. Power to the LCD can be

converted from 12V to 5V DC with a power converter, as shown on Figure 2, or sourced from the 5V pin on the Arduino. A master on/off power switch is also included, and a small push button wired in to control when the oxygen manipulation code begins ("start" button).

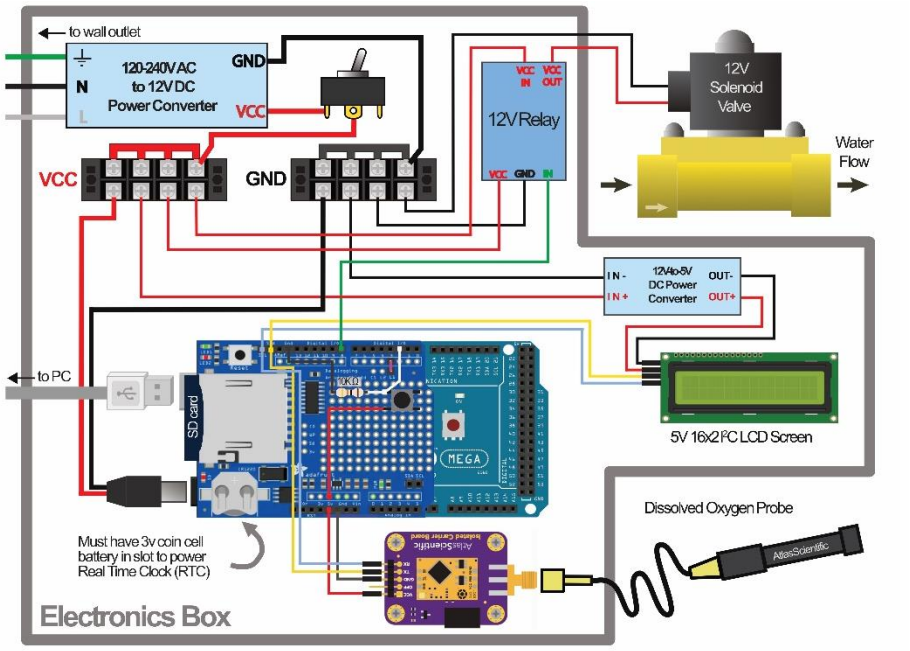

Figure 2. Wiring diagram. AC power from the grid is converted into DC power, shown as red (VCC) and black (GND) wiring. The VCC terminal block distributes power to each component, and the GND terminal block is a common ground to close the circuit. The Atlas Scientific EZO DO circuit and the LCD screen are controlled via I2C protocol from the SCL (clocking) and SDA (data) pins. The Arduino Mega 2560, SD shield, and LCD screen images are from https://fritzing.org/, and the Atlas Scientific EZO DO circuit image is from circuit documentation on https://atlas-scientific.com/.

When the code is started, it executes in repeated "loops"; within a single loop the system measures the DO in the tank, calculates the average DO over the last five readings, compares the average DO to the programmed DO, opens the valve to allow in oxygenated water if necessary, logs the data to the SD card, and displays the average and

planned DO on the LCD screen. The code may be restarted by pressing the "reset" button on the SD shield and then the wired-in "start" button. The average DO value is used rather than the instantaneous DO value to adjust for inherent noise in measurements, i.e., to prevent the system from allowing a single anomalously low measurement to trigger oxygenated water to flow in, even when the average DO is above the planned level.

Once the electronics have been assembled, construct the closed loop tank system (Figure 1). Three tanks are used in the system; the upstream reservoir tank for oxygenated water, the experimental tank in which study subjects are held and DO is manipulated, and a sump. Oxygenated water will constantly circulate between the reservoir and the sump, being intermittently diverted into the experimental tank whenever DO needs to be increased.

The reservoir tank and the sump may be made from simple plastic bins. Ideally, the experimental tank should be a clear aquarium tank so study subjects may be easily observed. Fit the experimental tank with an outflow standpipe and fill the tank with a layer of organic-rich sediment, which will consume oxygen and drive down DO in the overlying water. Fill the remaining space in the tank up to the top of the standpipe with seawater and allow suspended sediment to settle. Then, make two outflow holes in the reservoir tank. Attach a standpipe to the first hole and add plumbing to the outlet to direct overflow water into the sump. Attach the solenoid valve to the second hole and add piping or tubing to direct flow from the solenoid into the experimental tank. Position the reservoir tank above the experimental tank and fill the reservoir tank with seawater up to the standpipe. Place a sump pump in the sump and route tubing from its outflow up to the reservoir tank to close the loop.

Suspend the Atlas Scientific DO sensor in the experimental tank. The water's surface should be covered by a sheet of bubble wrap (which is oxygen-impermeable and will float at the surface) to prevent diffusion of atmospheric oxygen into the water. A small aquarium power head should be mounted in the experimental tank to gently circulate the water and prevent stagnation. In our setup with a 20 gal experimental tank, a 120 gph power head was sufficient. Manipulations by the Arduino are based on the readings from the sensor, so it is critical that the water is mixed such that the sensor readings represent the DO of the bulk water in the tank as accurately as possible. It is also important to note that if the system is to be used for rigorous experimental work, having all replicates in one tank presents the issue of pseudoreplication. To resolve this, multiple replicate experimental tanks should be plumbed and manipulated "in parallel", or if it is only feasible to have one experimental tank, multiple replicate trials performed over time.

1.5 Code

The annotated oxygen manipulation code and calibration code are freely accessible for download on the code sharing platform GitHub (kgadeken/OxygenManipulationCode_GadekenDorgan2021). It is highly recommended that new users read the code and annotations thoroughly before setting up and using the system.

1.6 Assessment

To serve as a usable method for manipulating oxygen in the lab, the system must reliably, precisely and accurately produce the programmed DO patterns in the

experimental tank. We tested the system by programming it to generate a diel oxygen cycle, with DO concentrations ranging from 3-7 mg L^{-1}. The diel cycle spans a wide range of DO values and demands the system adapt quickly to continually varying rates of DO change, therefore it is a highly rigorous test of the system's flexibility. Precision was gauged by the difference of each DO measurement from the programmed DO value at that time. To gauge the system's accuracy, we took corroborating oxygen measurements with an Onset HOBO DO logger. The Atlas Scientific probe and HOBO logger were both two-point calibrated immediately before starting the trial. The Atlas Scientific probe and the HOBO logger were secured in the experimental tank as close together as possible in the upper-middle of the water column at the same vertical height from the sediment surface. The HOBO logger was set to measure DO every 5 min.

Results from the diel cycle trial are shown in Figure 3. The system closely followed the diel pattern during rising and high DO periods but deviated slightly during falling DO. This indicates that the sediment was not consuming enough oxygen at these times to keep up with the programmed rate of decrease. At its greatest point, the difference between the measured DO and the planned DO was 0.91 mg L^{-1}. However, over 99% of the measurements taken deviated from the planned value by less than half of that maximum difference ($\pm$0.46 mg L^{-1}), and ~89% deviated by less than a quarter ($\pm$0.23 mg L^{-1}), indicating that the system typically followed the programmed pattern very closely.

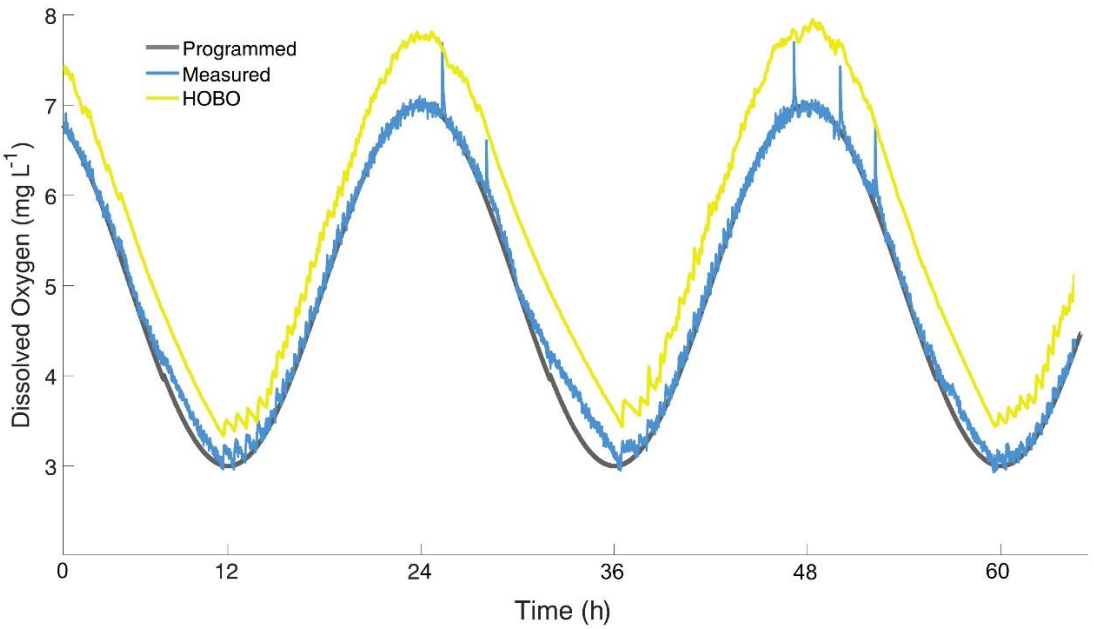

Figure 3. Results of testing of the oxygen manipulation system using a diel oxygen cycle (ranging from 3 mg L^{-1} to 7 mg L^{-1}). Precision was assessed from the difference between the measured DO (blue) and the programmed DO (gray) at each time point. An Onset HOBO DO logger (yellow) was included to take corroborating measurements every five minutes to assess the accuracy of the system's oxygen measurements and manipulation.

Because the HOBO was set to take measurements at 5 min intervals while the oxygen manipulation system measured DO every 37 s, values were interpolated from the HOBO sensor measurements to correspond to each of the measurements from the oxygen manipulation system. The HOBO measurements followed the same diel pattern as the system but were positively offset an average of 0.62 mg L^{-1}. The data from the oxygen manipulation system and the HOBO were both detrended and then analyzed for correlation, and no lag was found between the two data sets. Given this, it is likely that the difference between the sensor measurements is largely due to calibration error.

A potential critique of this setup lies in the use of sediment oxygen demand (SOD) as a DO sink. Using SOD rather than N_2 gas limits the rate of oxygen removal

from the water, as shown in the diel cycle trial during the periods of DO decline (Figure 3). Vigorous purging with N_2 gas or vacuum degassing can remove all oxygen from solution in seconds or minutes (Mount 1961), whereas our system using SOD typically takes several hours to decrease from full oxygen saturation to hypoxia. Low DO is also well known to be accompanied by a suite of related changes in sediment and water chemistry, altering chemical concentrations, changing nutrient fluxes and modifying pH (Froelich et al. 1979; Burnett 1997; Middelburg and Levin 2009). This is in contrast to the N_2 gas and vacuum degassing methods which strip DO by physically removing it from the water, and therefore do not result in the same chemical reactions as SOD. However, using sediments to scrub oxygen more closely resembles how low DO occurs *in situ*. Bubbling water with N_2 gas to remove oxygen also decreases the pCO_2 of the water, thus increasing pH, in contrast to oxygen consumption by sediments which typically decreases pH because organic matter remineralization generates CO_2 (Gobler et al. 2014). Though oxygen cannot be drawn down as quickly and the effects of change in DO alone cannot be as cleanly isolated with the SOD method because other chemical characteristics are unavoidably covarying, it more accurately represents DO variability as it would be encountered in natural settings. Also, because this system is closed-loop and relies on biological processes to function, issues with excessive buildup of ammonia and nitrates may arise if experiments are run for extended periods without replacing the water in the tanks. This system is best applied in situations that do not require independent control of water chemistry variables and for experiments that can be performed within a short time frame.

1.7 Modifications and Future Development

There are several ways that the user can modify the system to work more effectively or to troubleshoot issues. We divide these into "out-code" modifications, or changes to certain physical or structural features in the system, and "in-code" modifications, or changes to the Arduino code that alter the way the oxygen manipulation is executed.

1.7.1 Out-Code Modifications

The efficacy of the system depends heavily on the oxygen-consuming capacity of the sediments in the experimental tank. Use the most organic-rich sediments available and maximize the ratio of sediment surface area to bulk water volume by using as shallow a tank as possible. Before starting construction of the system, we recommend assessing the oxygen consumption rate the mud can achieve by putting mud into a tank with overlying water to the height anticipated for the experiment, adding a power head to circulate the water, covering the water with bubble wrap, and recording the oxygen through time. If the sediment is not consuming oxygen at a sufficient rate, adding labile organic matter or fertilizer to the sediment or displacing some of the overlying water with a solid object can help increase oxygen drawdown.

Although the power head in the experimental tank may be effective at laterally circulating water, there is still potential for vertical DO gradients to form in the tank, and the steepness of the gradient will increase closer to the sediment surface. Thus the positioning of the probe in the tank is important. The probe should be secured in position well above the sediment surface and close to the vertical level where study organisms will likely be located. Because the code manipulates DO based on the readings from only

one probe, it is also critical to take care in calibrating the sensor, as exemplified by the diel cycle trial (Figure 3). Before it is used the sensor should be two-point calibrated and its accuracy corroborated at multiple DO concentrations with measurements from a reliable instrument. Though the calibration held well in the diel cycle trial, during longer experiments we advise periodically comparing the DO concentration against a reliable measurement to check for sensor drift.

This system was devised for a study observing responses of sediment-dwelling organisms to changing DO, therefore the study organisms were kept in smaller replicate containers filled with sediment within the experimental tank. We constructed a platform that sat on stilts just above the sediment layer to support the replicate containers (Figure 1). This platform had as many gaps as possible so that the water at the sediment surface was well mixed.

1.7.2 In-Code Modifications

There are two main features of the code that may easily be altered to change the way that DO control is performed: the amount of time the solenoid is held open and the pause duration between loops.

If DO data are noisy and repeatedly jump substantially above the planned DO concentration, too much oxygenated water may be flowing in with each loop, and the amount of time the solenoid is held open should be decreased. Decreasing the duration between each loop changes the frequency that the DO is compared to the planned value and manipulated, essentially changing the sensitivity of the system. If this duration is too short, the power head in the tank may not have enough time to circulate high oxygen water added in the previous loop, resulting in inaccurate measurements and manipulation.

The time the solenoid is held open and the pause duration between loops work in concert to affect the precision of DO manipulation, and some amount of trial and error will be necessary to determine the optimal values for each. That said, the system has been shown to be somewhat resilient to changes in these variables. We performed a sensitivity test on the system, programming it to maintain DO at 5 mg L^{-1} for ~1.5 h four times, each with a different combination of the amount of time the valve is left open (either 3 s or 6 s) and the time between loops (either 20 s or 1 min) (Figure 4). In the four trials (3s:20s, 3s:1min, 6s:20s, and 6s:1min), the maximum deviation of the measured DO from the planned DO was 0.21, 0.27, 0.25, and 0.23 mg L^{-1} respectively. The percentage of time that the measured value deviated by less than half the maximum deviation was 80%, 91%, 82% and 81% respectively. All four trials effectively maintained the programmed DO concentration within a small range of variability.

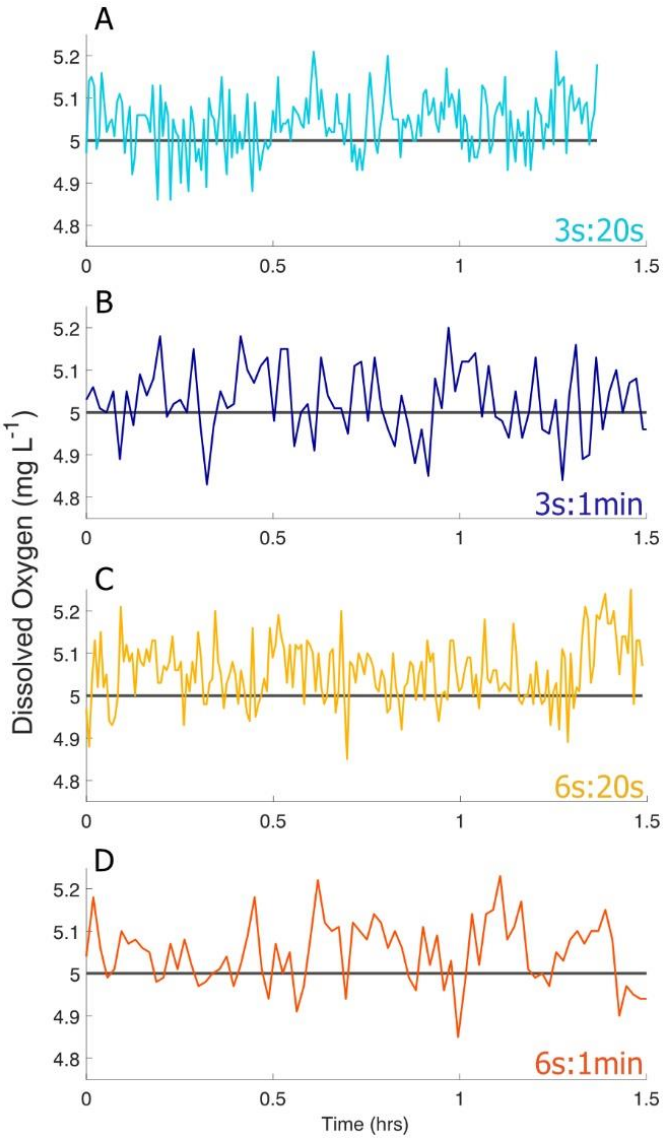

Figure 4. Results from sensitivity testing. The system was run four times, programmed to maintain DO at 5 mg L^{-1} (gray line) for ~1.5 h using different combinations of the amount of time the valve was held open, either 3 s (a and b) or 6 s (c and d), and the time waited between loops, either 20 s (a and c) or 1 min (b and d).

1.7.3 System Flexibility and Future Development

Aquatic organisms, particularly in coastal areas, exist in an environment with complex variations in DO that have long been difficult to reproduce in a lab setting.

Perhaps the most compelling prospect of the described system is its capacity to replicate this variation for study. The programmed oxygen pattern is controlled directly through the Arduino code to allow greater flexibility in the choice, combination and order of programmed patterns. For example, simply by adjusting the value or equation that the Arduino code is programmed to match and re-uploading the code, the system could be made to alternate increasing and decreasing DO at specific rates, allowing more rigorous study of how the rate of increase or decrease in oxygen affects animal behavior. Or, as was shown in the system test, it can produce a pattern from a modified sine function that mimics a diel oxygen cycle, an extremely common oxygen pattern in shallow coastal waters that remains understudied. The system could further be retrofitted with a high-pressure valve and small N_2 tank to supplement with N_2 purging when more rapid oxygen decrease is needed, or the oxygen probe upgraded to an optical sensor for more accurate and precise oxygen manipulation.

The system is also potentially useful for educational applications. It is designed to be as simple and modular as possible with readily available and reasonably priced components and relatively easy construction. Furthermore, using the code requires some familiarity with the Arduino programming language, and can serve as a model of how to use Arduino to build instrumentation for scientific inquiry. The system could be equally employed for classroom behavioral or physiological experiments and as a tool to teach experimental instrument fabrication.

CHAPTER II SEDIMENT MACROFAUNAL RESPONSE TO THE DIEL OXYGEN CYCLE

2.1 Abstract

Infauna exhibit a range of behavioral responses to declining dissolved oxygen concentrations that affect their burrowing and feeding behaviors. Diel oxygen cycles, common in shallow coastal areas, may drive changes in faunal behavior that affect sediment mixing on short temporal scales. In this study we exposed three faunal taxa (the burrowing ophiuroid *Hemipholis cordifera*, the tube-dwelling polychaete *Owenia fusiformis*, and the burrowing clam *Ameritella versicolor*) to a diel cycle of dissolved oxygen, observed them for behavioral changes, and evaluated their sediment mixing activity. We found that sediment mixing activity of all three taxa varies during the diel cycle but also decreases in response to repeated diel cycling. Observations of animal behavior did not reveal a diel pattern, though this was likely due to the temporal and spatial scale of observations. Our results suggest that diel cycling oxygen drives changes in faunal effects on the sediment that only emerge through repeated exposure. Investigating sediment mixing in full oxygen saturation or even sustained low oxygen may produce misleading estimates over time, and future estimations should consider how faunal responses to short-term variability can scale to have longer-term effects.

2.2 Introduction

Marine sediment infauna can dramatically change the physical and chemical structure of sediments. By burrowing through and feeding on sediments and irrigating

their burrow or tube structures, macrofauna mix solids and solutes into the sediments, which stimulates the sediment microbial community and drives increased nutrient cycling and organic matter breakdown (Aller 1978; Mermillod-Blondin et al. 2004; Mermillod-Blondin and Rosenberg 2006; Meysman et al. 2006). When dissolved oxygen (DO) in the water declines, these processes can be diminished or lost as sediment fauna experience severe stress or mortality from prolonged hypoxia (Diaz and Rosenberg 1995; Middelburg and Levin 2009; Sturdivant et al. 2012). However, in shallow coastal waters, DO patterns often follow a diel cycle as DO drops to hypoxic levels at night due to respiration and then increases during the day with photosynthesis, creating recurring but short-duration hypoxic conditions (Wenner et al. 2004; Tyler et al. 2009). When DO concentration is low, but not lethal, sediment macrofauna can alter their bioturbation and bioirrigation behaviors (Diaz and Rosenberg 1995; Riedel et al. 2014). Thus, diel-cycling DO may induce recurrent macrofaunal behavioral changes that affect their sediment mixing activity, particularly during the nightly period of the cycle.

Macrofaunal responses to stress can be diverse and complex. Early studies classified animals into one of two types, based on their strategy of dealing with low DO: oxyconformers, which adjust their oxygen consumption with decreasing DO, and oxyregulators, which keep their oxygen consumption independent of DO, to a certain level (Prosser 1973). These classifications have utility as broad descriptors; however, researchers have noted that they do not fully capture the gradations in response as oxygen changes (Prosser 1973; Mangum and Winkle 1973). Direct observations of infaunal species exposed to hypoxic conditions have shown a wide range of physiological and behavioral responses to decreasing and low DO, with effects often occurring in stages as

oxygen declines (Vismann 1990; Rosenberg et al. 1991; Nilsson and Rosenberg 1994; Diaz and Rosenberg 1995; Modig and Ólafsson 1998; Weissberger et al. 2009; Riedel et al. 2014). For example, the tube-dwelling polychaete worm *Diopatra cuprea* actively irrigates its tube with regular, rhythmic bursts of activity and the frequency of irrigation may not necessarily change linearly with oxygen concentration, i.e., after an initial decrease in irrigation rates upon encountering lowered oxygen saturation, some individuals maintain or even increase their irrigation rate as oxygen declines further (Mangum et al. 1968; Dales et al. 1970). This suggests that, on the time scale fauna would be most often encountering low oxygen, the diel scale, there may be undescribed complexity and variability in faunal behavioral responses. Taxa may vary in the severity of their responses to nightly low oxygen and in the time necessary to recover. With this variation in behavior and activity, we may expect corresponding differences in faunally mediated sediment mixing, a process that heavily influences sediment metabolism rates.

In this study we assessed whether and how infaunal behavior and sediment mixing activity vary with the diel oxygen cycle. We expected infauna to exhibit one of three hypothesized behavioral responses: a "proportional" response (H_1), wherein animal behavior and sediment mixing rates vary in direct proportion to DO concentration; a "gasp" response (H_2), wherein animals dramatically increase their activity to speed recovery when DO begins increasing from the nightly minimum; or a "lag" response (H_3), wherein animals are slow to recover from the nightly DO minimum.

We selected three infaunal taxa: a burrowing brittlestar (*Hemipholis cordifera*), a tube-dwelling polychaete (*Owenia fusiformis*), and a burrowing clam (*Ameritella versicolor*). These taxa were selected based on their local availability and because they

are all deposit/suspension feeders, thus their feeding behavior, e.g., time spent feeding, could be assessed for diel changes. Additionally, these taxa have different life histories, burrowing strategies, and physiologies that provided a range of attributes to gauge behavior and activity change. We expected that *H. cordifera* (family Ophiactidae) would increase the number of arms extended upwards to facilitate burrow ventilation and would cease excavating as DO declines in the diel cycle, and then dramatically increase excavation as DO rises in a gasp response. We expected that with declining DO *O. fusiformis* (family Oweniidae) would extend its crown upwards (respiring/suspension feeding) a greater proportion of the time rather than feeding on surface sediments or retracting into its tube and would defecate less frequently. We also expected that mixing activity would show a proportional response with diel cycling oxygen. Finally, we expected the small-bodied mobile burrowing clam *A. versicolor* (family Tellinidae) to decrease feeding and mixing activity with falling DO, and a spike in activity as DO begins to increase.

2.3 Materials and Methods

2.3.1 Study organisms

Hemipholis cordifera. Burrowing brittlestars are critical bioturbators in soft sediments. They live in excavated burrows and bury their oral discs several cm down, using some of their arms to anchor and extending others up out of the sediment to feed in the water column or sweep along the surface (Woodley 1975). The burrow is ventilated by an undulating motion in the upward-extended arms and this activity has been shown to drive

increased flux of oxygen into the sediment in the brittlestar *Amphiura filiformis* (Vopel et al. 2003). In sustained hypoxic conditions brittlestars do show signs of stress (reduced arm growth and spawning disturbance), however they can tolerate long periods of hypoxia without experiencing mortality (Nilsson and Skold 1996; Vistisen and Vismann 1997). Diel variation in *A. filiformis* activity, evaluated as the number of arms visibly protruding from the sediment, has been shown to be driven by photoperiod, increasing at night presumably so the animals avoid daytime predation by sighted predators (Rosenberg and Lundberg 2004). However, brittlestars have not to our knowledge been studied for responses to diel variation in DO. In shallow water DO and light typically covary, and increased brittlestar arm extension at night may be an irrigation response to declining oxygen.

Owenia fusiformis.The polychaete *Owenia fusiformis* constructs a shingled tube out of bits of shell and can actively alter the tube's position in the sediment (Eckman et al. 1981; Noffke et al. 2009). To feed, it extends its crown out of the tube and up into the water to catch floating particles or roves it about the sediment surrounding its tube (Dales 1957). *O. fusiformis* has demonstrated a high tolerance of sustained low oxygen by ceasing their activity (Dales 1958).

Ameritella versicolor. Burrowing clams are capable of impressive sediment reworking by actively burrowing through, feeding on and ventilating in sediments (Mermillod-Blondin et al. 2004). Clams are biodiffusive mixers, their activities resulting in random diffusive sediment transport as opposed to the directional transport of burrow- or tube-dwelling fauna (Michaud et al. 2005). The clam *Mya arenaria* has been shown to periodically expel water from its mantle cavity (pedal water ejection) in a cycle occurring on the order

of tens of minutes, oxygenating the surrounding sediment in pulses (Camillini et al. 2019a). Little is known about how the mixing or ventilation behaviors of clams change during low oxygen, though it is known that sustained hypoxia drives *Macoma balthica* to decrease its burial depth (Long et al. 2008), and one of the few existing studies on the faunal effects of diel cycling oxygen revealed diminished growth and survival in larval and juvenile bivalves when in combination with diel varying pH (Gobler et al. 2014). There is little existing information on the habits of our study species, *A. versicolor*, however we expected its general feeding and burrowing behaviors to resemble other well studied burrowing clam taxa.

2.3.2 Animal and sediment collection

Sediment and study animals were collected from Petit Bois Pass (30.231385º, -88.373072º), between Dauphin and Petit Bois islands, in Alabama, USA on April 27, 2020. The collection site was ~5 m depth and had a salinity of 25 psu. Animals were brought back to the lab and temporarily held in large tupperware containers filled with sediment from the collection site, submerged in aerated seawater at 25 psu.

Sediment was hand-sieved to remove large infauna, then thoroughly homogenized in a kitchen blender to eradicate small infauna. The blended sediment was used to fill 16 microcosms, i.e., thin, transparent aquaria for viewing infauna from the side (internal dimensions, 10.2 cm x 10.2 cm x 1.2 cm). The sediment was allowed to settle for two days and then topped off with more blended sediment so that the sediment-water interface was roughly even with the top edge of the microcosm. Filled microcosms were placed in a large holding tank with seawater (25 psu) in the lab for four days and allowed to settle and develop visible redox layering. Then, animals were removed from

tupperware containers and one individual potted into each of four replicate microcosms for each taxon. Four microcosms were left with only sediment for a control treatment. Microcosms were then returned to the bubbled holding tank and kept there until use in an experimental trial.

2.3.3 Exposure setup

The laboratory setup for the oxygen exposure is described in detail in Gadeken and Dorgan (2021). DO was manipulated in a diel cycle in the lab using a custom-built Arduino-based controller integrated into a closed loop aquarium system, hereafter called the "Oxygen Manipulation Machine" (OMM) (Figure 5). An experimental tank (76 L clear aquarium) held the microcosms, and a layer of organic-rich mud at the bottom of the tank consumed oxygen. A sheet of oxygen-impermeable bubble wrap was placed on the surface of the experimental tank to prevent oxygen exchange with the air. When the DO in the tank dropped below a pre-programmed level, a valve opened and allowed oxygenated water to flow in from an upstream reservoir tank, adjusting the DO in the experimental tank through time to match the programmed pattern.

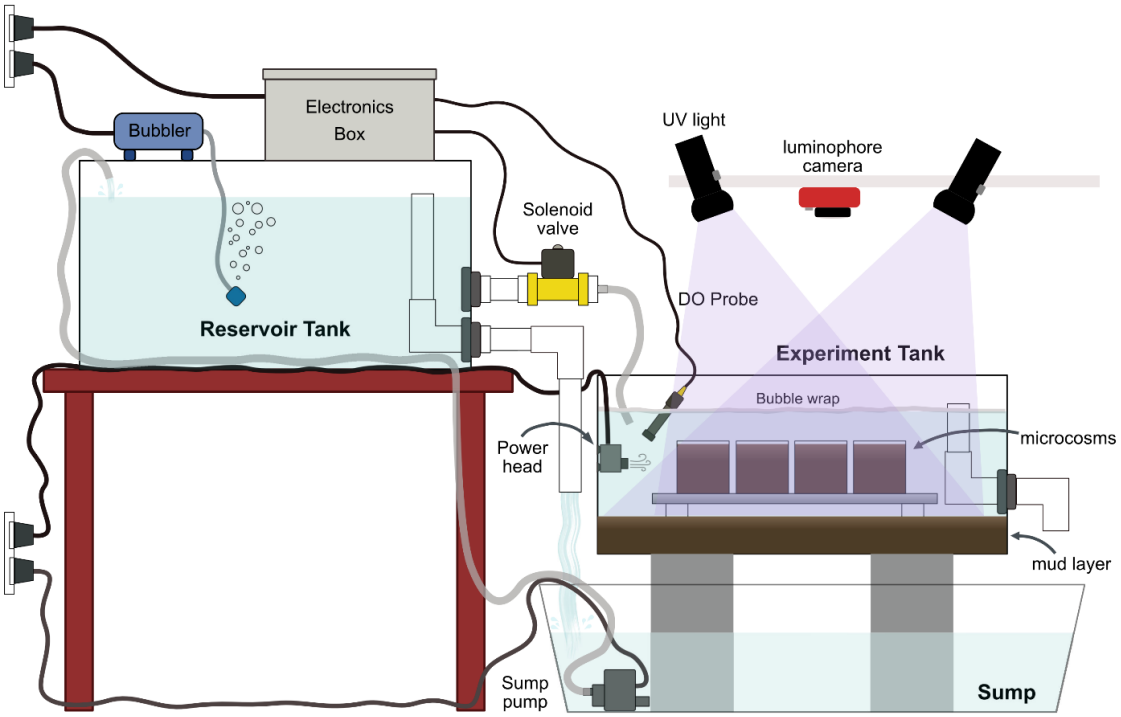

Figure 5. Oxygen Manipulation Machine (OMM) schematic (after Figure 1 in Gadeken and Dorgan 2021). The electronics box contained an Arduino microcontroller and an Atlas Scientific EZO DO circuit, hooked up to the DO probe in the experimental tank. A layer of organic-rich mud in the bottom of the experimental tank consumed DO. The Arduino was programmed to take periodic DO readings via the probe, and when DO was sensed to be below the pre-programmed level for that time due to oxygen consumption by the mud, the solenoid valve was opened and oxygenated water from the reservoir tank allowed to flow in to increase the DO. Microcosms were placed on a raised platform in the experimental tank, and the water surface covered with bubble wrap to prevent oxygen exchange with the air. At measurement points throughout the trials, the UV lights were turned on and pictures were taken with a downward-facing luminophore camera mounted above the tank.

The experimental tank could not hold all the microcosms simultaneously and allow for visualization and photos of each tank, so the experiment was run in four replicate trials with one replicate of each animal treatment in the experimental tank for each trial. During each trial the OMM was programmed to execute two full diel oxygen cycles, with 6 hr periods of sustained high and low oxygen at the beginning and end of

the trial, respectively (Figure 6). These periods were included to provide baselines of animal behavior to which behavior during the diel cycles could be compared. This resulted in three 12 hr periods of declining DO and two 12 hr periods of increasing DO in each trial. All trials were begun late at night in real clock time so that the DO minimums of the diel cycles occurred in late afternoon. This was done so that the most sampling-intensive period of the trials occurred during daylight hours to ease data collection. The level of high DO was set as 7 mg L^{-1}, just under the calculated oxygen solubility concentration (7.17 mg L^{-1}) at the average experimental salinity (25 ppt) and temperature (25 ºC); the low DO concentration was set at the widely accepted threshold for hypoxia, 2 mg L^{-1} (Rosenberg et al. 1991). After each trial a small amount of fresh mud was added to the sediment at the bottom to replenish the sediment organic matter and encourage DO consumption and 50% of the circulating system's water was exchanged to prevent buildup of toxic metabolites.

2.3.4 Sediment mixing

Changes in sediment mixing throughout the trial were assessed using luminophores – sediment particles covered in fluorescent paint (Solan et al. 2004; Dorgan et al. 2020). The luminophores were dry sieved through a 250 µm and then a 63 µm sieve, and particles retained on the smaller sieve (fine to very fine sand) used in the experiment. A thin layer of luminophores ~ 0.5 mm thick was applied to the surface of the sediment in the microcosms and pictures taken at specific measurement points during each experimental trial (blue points in Figure 6). To take pictures, the bubble wrap covering on the experimental tank was briefly pulled aside, the overhead room lights were turned off and UV lights shone at an angle onto the sediment surface to illuminate

the luminophores. Pictures were taken using a horizontally mounted camera with a top-down view of the microcosms.

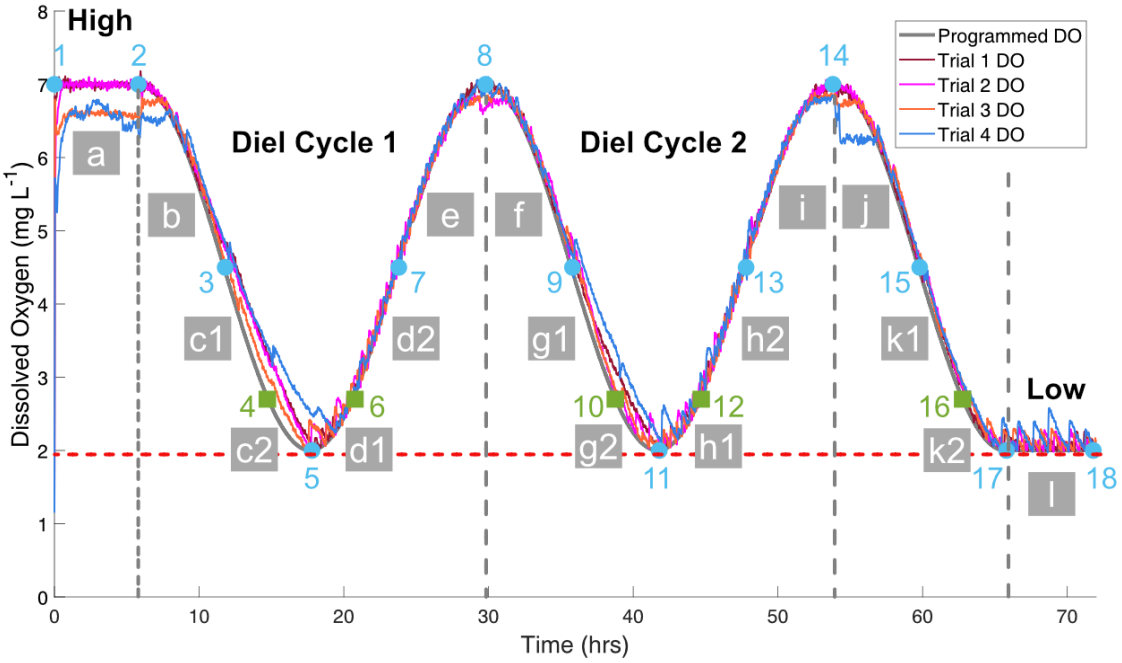

Figure 6. Patterns of DO manipulation in the experimental trials. The OMM was programmed to execute two diel cycles with 6 hr periods of high and low DO at the beginning and end of the trial, respectively (black line). High DO concentration was set as 7 mg L^{-1} and low concentration as 2 mg L^{-1} (red dotted line). Blue circle points indicate when top-down pictures of luminophores were taken and new luminophores were applied. Green square points indicate when pictures were taken but luminophores were not applied. Lettered grey boxes denote the measurement intervals.

Preliminary observations revealed that infauna can remove most luminophores from the sediment surface surrounding their tube or burrow openings within a few hours. To allow for repeated estimations of mixing activity throughout the multi-day trials, at the beginning of each measurement interval (grey lettered boxes in Figure 6) additional luminophores were applied to areas of the sediment where most particles had been mixed

down to re-cover the sediment, and an additional picture taken of the sediment surface. Then, initial pictures could be compared with final pictures for each interval to measure mixing activity during that interval (Figure 7). At all mid-low points (Figure 6, points 4, 6, 10, 12, and 16), pictures were taken but new luminophores not applied.

Measurement points were selected as the minimum, maximum, and midway points on the diel cycles as well as additional points just before and after the minimum DO. These extra points in the trough of the diel cycle (mid-low points) were included to better capture possible "gasp" or "lag" responses as DO just begins to increase from minimum. Mixing activity could, for example, be compared between interval *c2* and interval *d1* (Figure 6) to determine if activity differs for the same DO concentrations when DO is falling vs when it is rising.

Note that mixing activity is not a direct measure of bioturbation, which would require destructive sampling of sediments and preclude repeated measurement. It also alone cannot capture directionality of sediment mixing as a sediment surface where luminophores have been subducted looks similar in top-down photos to a sediment surface where luminophores have been covered with sediment excavated from depth. However, it does serve as a useful proxy for mixing intensity and allowed for repeated measures of activity for the same animal as DO varied.

Early in trial 3 we noticed tracks in the surface sediments of the control treatment microcosm, and at measurement point 8 we extracted a small burrowing snail from the sediment. During data analysis we discarded the mixing activity measurements of that replicate from intervals before the snail was removed. Also, the flow control mechanism on the power head in the experimental tank (Figure 5) malfunctioned at the beginning of

trial 3 and caused increased flow in the tank that appeared to remove luminophores from the top sediment layer of the microcosms. The flow control was repaired at measurement point 2 and mixing activity data from interval *a* of that trial was not used in analysis (Figure 6).

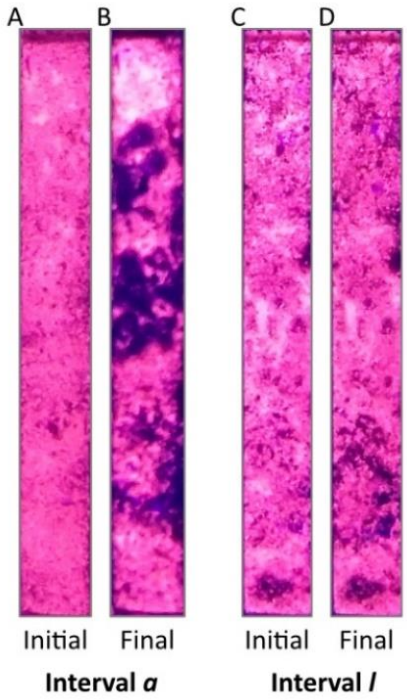

Figure 7. Examples of top-down luminophore pictures analyzed for mixing activity. (A) and (B) are the initial and final pictures taken of the microcosm in trial 2 containing *Ameritella versicolor* in sustained high DO (interval *a* in Figure 3), and (C) and (D) are initial and final pictures of the same microcosm in sustained low DO (interval *l* in Figure 3).

Luminophore pictures were analyzed using the image analysis software ImageJ (Rasband 2018). Images were cropped to contain only the microcosm sediment surface (Figure 7), auto-contrasted to standardize brightness, converted to 8-bit, segmented using

a brightness threshold to isolate the area covered by the luminophores (brightness: 70-255), and percent cover calculated. Mixing activity during each measurement interval in the trial was calculated as the difference between percent luminophore cover at the beginning and end of the interval. Changes in mixing activity throughout the diel cycle were evaluated by comparing the change in percent cover between measurement intervals using a pairwise Mann-Whitney U test, and differences in mixing activity between the animal treatments and the control were assessed using a Kruskal-Wallis test with a Bonferroni correction for multiple comparisons. Overall patterns throughout the trials were assessed by fitting polynomial curves through all values for each treatment with DO concentration and the elapsed time in the trial as predictive variables. Analyses were performed in Matlab 2021a (The MathWorks Inc. 2021).

2.3.5 Animal behavior

Animal behavior and activity were monitored with time-lapse photographs of the microcosms. GoPro Hero4 cameras with attached macro lenses were mounted outside the tank, positioned with a view at each of the microcosms containing animals through the tank wall. Room lights were kept on during all trials to allow for clear photography and to control for effects of lighting on behaviors. The cameras were programmed to take time-lapse photos once per minute for the duration of each trial and were compiled into a video for further analysis. Video segments were excluded at each measurement point because the lights were turned off to take photos of luminophores, and a portion of the video of the *Owenia fusiformis* in trial 3 (amounting to ~5 hrs of real time) was lost due to camera malfunction.

Animal behavior was quantified using the open-source event-logging software BORIS (Friard and Gamba 2016). An ethogram of animal behaviors was constructed for each taxon (Table 2) and videos were examined frame-by-frame and coded for presence or absence of ethogram behaviors.

Table 2. Behaviors used for ethography. Behaviors marked with a (*) are point events, all others are state events.

Taxon	Behavior	Description
Hemipholis cordifera	Excavation	Sediment from depth is deposited on the sediment surface
	Arms Extended (1-5)	Number of arms extended out of sediment
Owenia fusiformis	Crown Retracted/Not Visible	Worm crown retracted into its tube, or the crown can't be seen
	Crown Up	Respiring and/or suspension feeding (crown extended upwards)
	Crown Down	Deposit feeding (crown repeatedly bent down to sediment surface)
	Defecation*	Production of fecal pellet at sediment surface
Ameritella versicolor	Irrigating/ventilating	Sediment is visibly pulsing upwards from clam ventilation
	Change Location*	Focal point of pulsing sediment shifts elsewhere in the ant farm
	Feeding	Siphon(s) are visible probing through sediment

For analysis, the event logs of all coded videos were exported from BORIS as binary tables binned in three-minute (real-time) intervals. We calculated the proportion of time each animal spent performing the different behaviors for each 6 hr interval of the exposure (blue measurement points in Figure 6) and performed a Kruskal-Wallis test with

a Bonferroni correction to compare these values between all the intervals and determine if behavior changed between when DO was falling and rising in the diel cycle.

2.4 Results

The DO in the experimental tank followed the programmed pattern in all four trials (Figure 6). In trial 4, DO declined slightly slower than was necessary to keep pace with the programmed pattern in the trough of the first diel cycle, likely because the layer of mud consuming DO in the tank was becoming depleted in organic matter. However, DO dropped to 2.25 mg L^{-1} at the lowest point of the first cycle and showed improved performance in the second.

2.4.1 Sediment mixing

Most mixing activity values were negative or close to zero, indicating that percent luminophore coverage during those intervals either decreased or did not change (Figure 8). Sediment mixing in the control treatments remained low and stable for the duration of the trial (Figure 8A).

Downward sediment mixing in all three animal treatments was highest and most variable in the high DO period at the beginning of each trial, generally decreasing in variability as the trials went on. No animal treatments differed in mixing activity from the control treatment in the beginning sustained high DO period (interval *a*), though this was likely due to the small sample size from excluding data from trial 3 (Kruskal-Wallis with Bonferroni correction, $p > 0.05$). By the low DO period at the end of the trials (interval *l*) animals appeared to be doing very little mixing, though *Ameritella versicolor* had

significantly greater mixing rates than the control in that interval (Kruskal-Wallis with Bonferroni correction, $p = 0.03$).

In the first diel cycle *Hemipholis cordifera* showed significantly greater mixing just after the DO minimum than before (intervals *c2* and *d1*, Mann-Whitney Wilcoxon, $p = 0.03$), though this was not the case in the second diel cycle (intervals *g2* and *h1*, Mann-Whitney Wilcoxon, $p = 0.34$) (Figure 8B). There was no difference between mixing activities in *H. cordifera* in the declining and rising mid-low intervals in either cycle (intervals *c1* and *d2* (Mann-Whitney Wilcoxon, $p = 0.86$), and intervals *g1* and *h2* (Mann-Whitney Wilcoxon, $p = 0.34$)). For both *O. fusiformis* and *A. versicolor* there were no differences in the mixing activities before and after the DO minimums, nor were there differences between the mid-low intervals in either diel cycle (Mann-Whitney Wilcoxon, all $p > 0.1$) (Figures 8C and 8D).

All three animal treatments displayed a similar pattern of decreased mixing throughout the trial, punctuated by variation with the diel cycles. A polynomial curve was fit to the data for each taxon:

(1) $$L = ax + bt^c + d$$

where L is percent luminophore coverage (i.e., mixing rate), x is DO concentration, t is the time in the trial, and a, b, c, and d are the term coefficients. In this equation, the first term (ax) is the variation due to DO concentration, and the second term (bt^c) expresses the overall decrease in mixing throughout the entire time of the trial. The values for each term coefficient and their 95% confidence intervals were calculated for the animal treatments and the control. The coefficients, and therefore the terms in the function, were

deemed statistically significant if the confidence interval did not include zero. Change in the control treatment mixing rate throughout the trial was not well explained by the

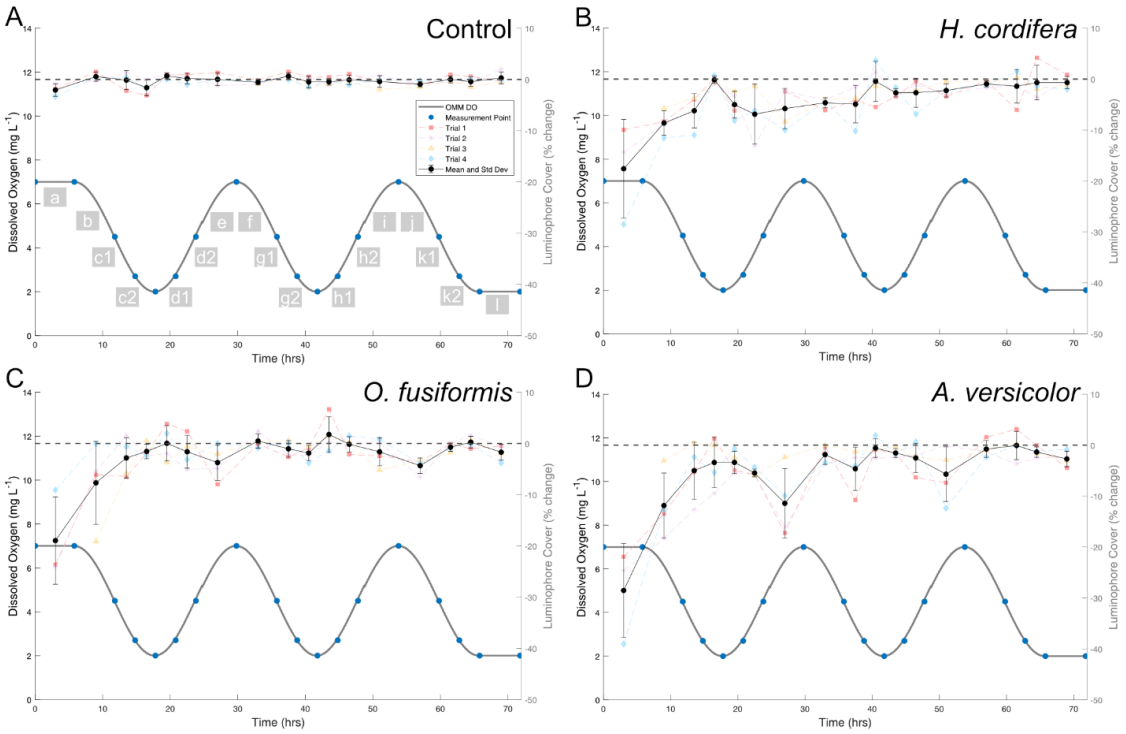

Figure 8. Sediment mixing activity (right y-axis) for (A) Control, (B) *Hemipholis cordifera* (brittlestar), (C) *Owenia fusiformis* (polychaete worm), and (D) *Ameritella versicolor* (clam), throughout the trials, expressed as the change in percent of the sediment surface covered by luminophores in the microcosm throughout each interval (i.e., a negative value indicates luminophore cover had decreased over that interval). The average percentages and their standard deviations for each interval are plotted in black, with the data points for individual replicates in each trial shadowed behind them. The lettered grey boxes denoting the intervals have been included on (A) for ease of reference with the text, and the DO pattern programmed into the OMM and measurement points plotted on each to compare mixing activity throughout the trials (left y-axis). Blue dots on DO time-series show when pictures of luminophores were taken.

function (no significant coefficients), while mixing rates in *O. fusiformis* and *A. versicolor* were significantly explained by both DO concentration (coefficient *a*) and the

time in the trial (coefficients *b* and *c*) (Table 3). *H. cordifera* mixing rates were significantly explained by time in the trial, but not DO concentration (Table 3).

Table 3. Values and confidence intervals of function coefficients. Those values shaded in grey are the coefficients of the DO and time terms in the function $L = ax + bt^c + d$. * indicates significant coefficients (the confidence interval does not include zero).

Taxon	*a*	*b*	*c*	*d*
Control	-0.03 ± 0.17	$-6.12e^3 \pm 1.85e^7$	$-7.49 \pm 2.76e^3$	-0.06 ± 0.68
Hemipholis cordifera	-0.47 ± 0.52	-31.67 ± 13.57*	-0.54 ± 0.53*	3.40 ± 7.64
Owenia fusiformis	-0.57 ± 0.51*	-63.16 ± 49.70*	-1.20 ± 0.70*	1.78 ± 2.62
Ameritella versicolor	-0.81 ± 0.64*	-70.33 ± 38.36*	-0.94 ± 0.49*	2.26 ± 4.15

2.4.2 Animal behavior

Hemipholis cordifera.In three of the *H. cordifera* replicates the subsurface view of the animal through the microcosm wall was mostly obscured by sediment, however the individual in trial 1 was completely visible, allowing for direct observation of its below-ground activities and description of behaviors. The animal maintained a large, excavated space at depth for positioning its anchoring arms and oral disc, and pink luminophore particles could be seen at depth in the burrow, indicating subduction or collapse of sediments from the surface (Figure 9A). During burrow excavation, the animal transported sediment with its tube feet, conveying sediment particles up the anchoring arm, around its oral disc and up an extended arm to deposit it in a pile at the surface. The animal also frequently reorientated its body by rotating its oral disc and shifting its arms, often moving an upwardly-extended arm down to anchor or an anchoring arm upwards into the water column. All *H. cordifera* buried their central discs in the microcosms and

remained buried throughout their experimental trials, extending their arms up into the water column and occasionally excavating sediment into piles around their arm holes. There was no difference in amount of time spent excavating between any of the time intervals throughout the trial, nor were there significant differences in the number of arms extended into the water column (Kruskal-Wallis with Bonferroni correction, $p > 0.05$) (Figure 9B).

Owenia fusiformis. The crowns of all *O. fusiformis* individuals could be observed in the time-lapse videos (Figure 5C), and we observed the worms bending their crowns down to surface sediments to deposit feed. Frequently, a worm retracting its crown into its tube was followed by defecation. We also observed several instances of the worms rapidly moving upwards, partially unearthing their tubes and extending their crowns further up in the water column.

There was considerable variability between *O. fusiformis* individuals both in the amount of time spent performing the different behaviors and in the timing of behaviors throughout the exposure (Figure 9D). We found no significant differences in the proportion of time spent deposit feeding or suspension feeding throughout the trials (Kruskal-Wallis with Bonferroni correction, $p > 0.05$).

Ameritella versicolor. Though the clam's shells were buried and were not visible most of the time, we could easily observe them foraging through the sediment with their siphons (Figure 9E). There was also a notable pulsing motion occurring in the top layer of sediment, which we interpreted as the clam ventilating and irrigating the surrounding sediments, and in some trials the focal point of this pulsing would relocate elsewhere in the microcosm. In trials 1, 2 and 3, irrigation was consistently observed throughout the

entire trial duration, and in trials 2 and 4 feeding was consistently observed (Figure 9F). There were no statistical differences between irrigation and feeding activity at the different measurement intervals throughout the trials (Kruskal-Wallis with Bonferroni correction, $p > 0.05$).

2.5 Discussion

The diel variation and similarity of mixing activity in falling vs rising DO in *Owenia fusiformis* and *Ameritella versicolor* indicate that these taxa tend to exhibit a proportional response (H_1) to the diel cycle. *Hemipholis cordifera* did exhibit greater mixing after the DO minimum in the first diel cycle which suggests a gasp response (H_2), however this response was diminished in the second diel cycle as overall mixing rates trended towards zero. More generally, sediment mixing declined and stabilized throughout each trial, decreasing from the high and variable levels in the high DO interval at the beginning and approaching zero in the declining and low DO conditions at the end. This indicates that not only are animals responding to changing DO, but they are adjusting to mixing sediments less intensely than what is observed in high or saturated DO conditions. It is also notable that for all three animal treatments, mixing activity declined exponentially throughout the trial and over the two replicate diel oxygen cycle exposures, and mixing activity for *H. cordifera* showed no variation with the diel oxygen cycle. It appears that for these animals, repeated exposure to the diel oxygen cycle overall drives mixing

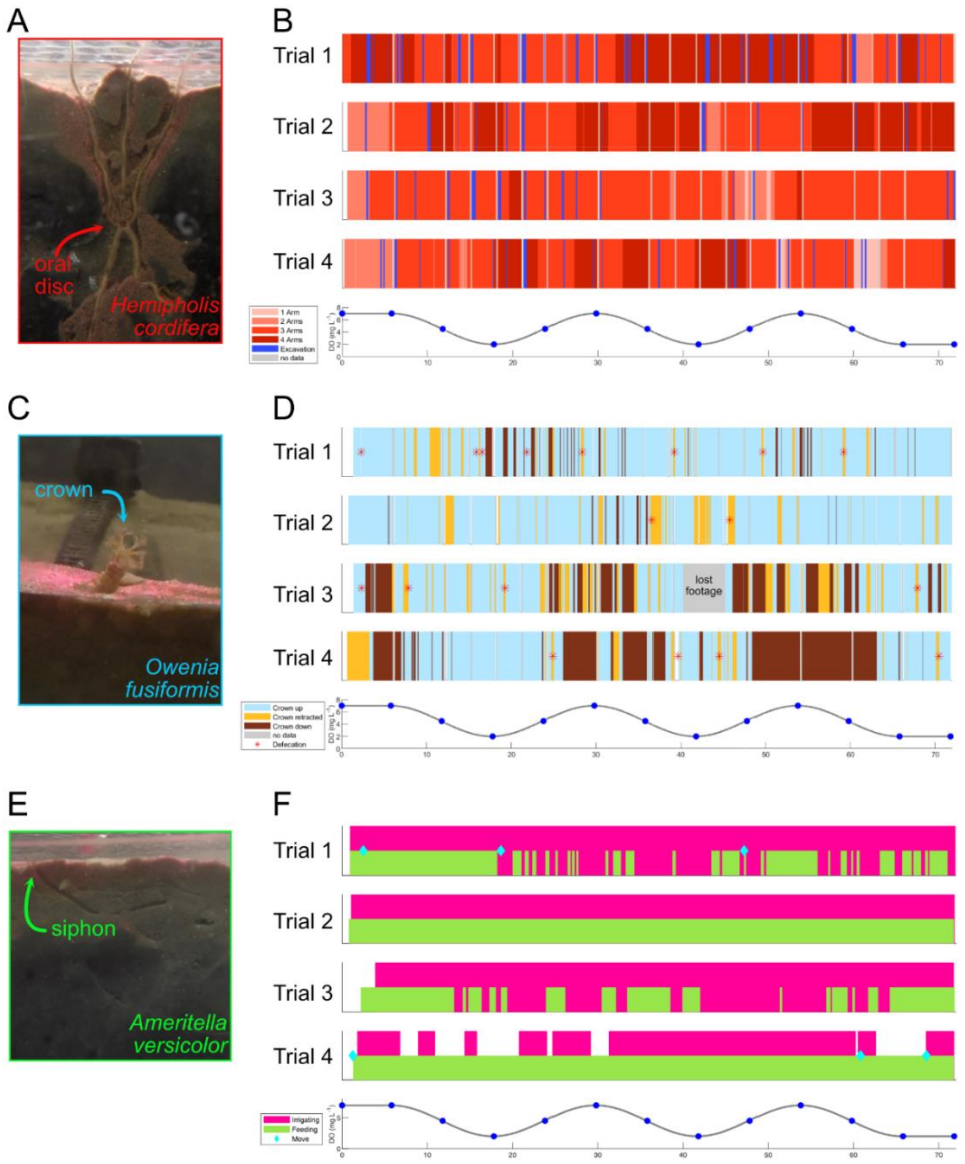

Figure 9. Images of animals in microcosms and coded behavior patterns throughout the four trials for each of the three study taxa. *Hemipholis cordifera* anchors its body with some of its arms while stretching the others up into the water column to feed. In trial 1, the entire animal was visible through the side of the microcosm (A). Pink luminophore particles could be seen at depth, indicating surface sediments had been subducted or collapsed into the burrow. (B) Shows the variation in the number of arms elevated above the sediment and the timing of excavation events. (C) *Owenia fusiformis* extends its crown up into the water column to suspension feed or respire and (D) repeatedly bends its crown down to the surface to deposit feed and retracts it into its tube when defecating. (E) *Ameritella versicolor* tunnels its extendable siphon through the sediment to feed, and though the shell is not usually visible, in (F) a pulsing motion can be observed in surface sediments as the animal ventilates. The location of this pulsing occasionally changed during the trial for some individuals.

activity down, dampening it even at points in the cycle when DO is high. This raises an intriguing question of whether further repeated exposure to diel oxygen variation would continue to drive mixing activity down or if instead it would stabilize, with a diel-driven proportional response still occurring albeit at a diminished magnitude.

Given the apparent change in mixing activity throughout the trials, it was surprising that no corresponding behavioral patterns were observed for any of the taxa. Behavior patterns were highly variable between replicates within taxa which may have obscured the effect of changing DO. However, it is more likely that faunal behaviors relevant for comparison to mixing activity varied on a shorter temporal scale or via more nuanced behavioral shifts than our time-lapse imaging was able to capture. In both *H. cordifera* and *O. fusiformis*, suspension feeding and respiration occur in similar postures and are not easily differentiated through image analysis which may have obscured important behavioral shifts as DO varied.

The ventilation behavior observed in *A. versicolor* is consistent with behavior observed in a larger bivalve species (Camillini et al. 2019b), however it appeared to occur far more rapidly; sediment pulses often took place over one or only a few minutes (Video S6). The clams also ventilated consistently throughout our trials (Figure 9C) which indicates that DO variation may not determine whether the clams ventilate but rather the frequency and amplitude of ventilation.

Most laboratory studies on the mixing of sediments by fauna make no mention of the DO concentrations in their experimental setups, but presumably DO was maintained at high or saturated levels for the duration of the experiments (Pelegri and Blackburn 1995; Widdicombe and Austen 1999; Mermillod-Blondin et al. 2004; Michaud et al.

2005). Those studies that focus on faunal responses to low oxygen typically expose the animals to sustained conditions of different treatment DO concentrations (e.g., high vs low) (Seitz et al. 2003; Weissberger et al. 2009; Calder-Potts et al. 2015), or if variable DO is included, it is as an exposure in unidirectional declining oxygen (Dales et al. 1970; Kristensen 1983; Riedel et al. 2014), equivalent to taking measurements up to the minimum DO of the first diel cycle in our trial pattern. Our results suggest that measurements of sediment mixing by fauna in sustained high DO may produce overestimations of long-term mixing rates, particularly for animals that, in *in situ* conditions, would be experiencing variable DO. Additionally, it may require more than a single exposure to declining DO, more even than a full diel cycle, for behaviors to emerge and stabilize into a repeating pattern that may be representative of *in situ* responses. Short-term variability and the responses it induces can scale to have longer-term effects, and better describing this linkage is critical to improving both conceptual and numerical models of dynamic coastal systems.

CHAPTER III AN IN-SITU BENTHIC CHAMBER SYSTEM FOR HIGH-RESOLUTION MEASUREMENT OF SEDIMEND OXYGEN DEMAND THROUGHOUT A DIEL CYCLE

3.1 Abstract

Sediment oxygen demand is affected by dissolved oxygen concentrations and by the activities of sediment macroinfauna, both of which can vary over short time periods in shallow coastal systems. Prevailing methods to measure sediment oxygen demand *in situ* generally require measurement periods that are too long in duration to capture the temporal variability in SOD driven by diel cycling of dissolved oxygen concentrations. These techniques also preclude linking changes in SOD to sediment faunal activities, which can change on short time scales and can also be affected by ambient oxygen concentrations. Here we present an *in situ* instrument to repeatedly measure sediment oxygen demand in discrete areas of sediment throughout a diel oxygen cycle. The system isolates patches of sediment and the resident fauna in replicate benthic chambers, and measures and records oxygen decrease for a short time before refreshing the overlying water in the chamber with water from the external environment of ambient DO concentration. This results in a sawtooth pattern in which each tooth is an incubation, providing an automated method to produce direct measurements of *in situ* sediment oxygen demand that can be directly linked to the macrofaunal community composition.

3.2 Introduction

Sediment oxygen demand (SOD) is a crucial metric for assessing the health and function of marine ecosystems (Diaz and Rosenberg 1995; Middelburg and Levin 2009). High respiration rates in shallow, organic-rich sediments make them a major sink of oxygen, and animals living in sediments (benthic macrofauna) increase oxygen drawdown by burrowing through, feeding on and irrigating sediments (Aller 1978; Norling et al. 2007). High dissolved oxygen (DO) concentrations promote healthy food webs and organic matter (OM) remineralization, whereas hypoxia (DO < 2 mg L^{-1}) slows OM decomposition and causes mortality of macrofaunal organisms (Diaz and Rosenberg 1995; Middelburg and Levin 2009).

Persistent hypoxia dramatically affects ecosystem health, but low DO in coastal environments often occurs on much shorter timescales (Wenner et al. 2004). DO concentrations in shallow productive waters often follow a diel cycle with high DO concentrations during peak light periods due to high photosynthesis rates and low, often hypoxic concentrations during dark periods driven by high respiration (Tyler et al. 2009). Sediment communities have been intensively studied under sustained normoxic and hypoxic conditions (Herreid II 1980; Diaz and Rosenberg 1995; Diaz 2001; Levin et al. 2009; Middelburg and Levin 2009; Foster and Fulweiler 2019), but much less is known about how such short-term oscillations in DO concentrations impact SOD. For example, when DO concentration is low, but not lethal, sediment macrofauna often alter their bioturbation and bioirrigation behaviors (Diaz and Rosenberg 1995; Weissberger et al. 2009). There is little research on macrofaunal behavioral responses to diel cycling DO or the effects of their behaviors on SOD throughout the cycle.

This lack of knowledge can in part be explained by the methodological challenges of measuring SOD, particularly *in situ*. A long-used method of measuring chemical fluxes in sediments in the field is the "batch style" (completely enclosed) benthic metabolism chamber, commonly deployed once or a few times in a day (Tengberg et al. 1995). Because it must be manually deployed for each SOD measurement, the batch metabolism chamber generates very low temporal resolution of SOD data and usually restricts measurements to daylight hours, or the time in the daily cycle when DO is highest. However, it does allow SOD measurements to be associated with discrete areas of sediment and the burrowing and irrigating animal community within, and it captures spatial variability when used with sufficient replication.

More recently, the eddy-correlation technique, used for decades to measure fluxes in the atmospheric sciences, has been adapted for use in aquatic systems to collect *in situ* measurements of SOD (Berg et al. 2003). With this technique, SOD for a given area of sediment is calculated from point measurements of dissolved oxygen and the velocity field taken above the sediment surface. This allows for measurement of SOD at a far higher temporal frequency than is typical with benthic chambers, enough to capture diel variability (Berg et al. 2019). Another distinct advantage is the open design; unlike benthic chambers, eddy correlation does not require enclosure of a portion of sediment and thus does not obstruct natural flow conditions. However, this means that natural variability in flow rates and directions change the size and shape of the sediment area contributing to the flux, so eddy correlation is most appropriately viewed as a spatially-averaged flux measurement technique. Sediment macrofaunal behaviors typically influence SOD in a highly localized volume around their tube or burrow structure (Zorn

et al. 2006; Volkenborn et al. 2010), and eddy correlation lacks the spatial resolution to determine how different macrofaunal taxa affect SOD.

The existing methods to measure SOD *in situ* are optimized to either capture temporal or spatial variability but are insufficient to describe the relationship between the two. We have built a system to capture better temporal resolution throughout the daily oxygen cycle than single-deployment batch chambers, and better spatial variation in macrofaunal effects than eddy correlation technique. This setup and methodology will allow for improved description of the complex relationship between DO concentration, macrofaunal activity, and metabolism in shallow sediments.

3.3 Materials and Procedures

The system is designed to take repeated measurements of SOD in replicate benthic chambers (Appendix A, Figure A1) and is comprised of a central housing for power and electronics and five chambers that are tethered to the central housing (Figure 10A). The central housing for power and electronics (Figure 10B, Appendix A, Figure A2) controls submersible pumps attached to the chambers (Figure 10C) and is programmed to periodically turn on each chamber pump (Flush Pumps) for a short time to flush the overlying water with water of ambient dissolved oxygen concentration from the environment. DO is measured in each chamber by an Onset HOBO DO logger, and SOD can be found from the slope of the decrease in DO in each measurement period. Over an entire deployment, this results in the DO within the chambers following a sawtooth pattern, with the slope of each tooth being an SOD incubation (Figure 11). To mix the overlying water and prevent stagnation in between water exchanges, a small,

enclosed impeller was outfitted with two neodymium magnets (0.375" W x 0.125" H) arranged with opposite polarity to magnetically couple with a stirbar (5/16" OD x 1" L) through the chamber lid. When water is pumped through the impeller enclosure, the Impeller spins, mixing the water in the chamber. A single pump (Mixing Pump) plumbed in series with five benthic chambers provided all mixing actions simultaneously.

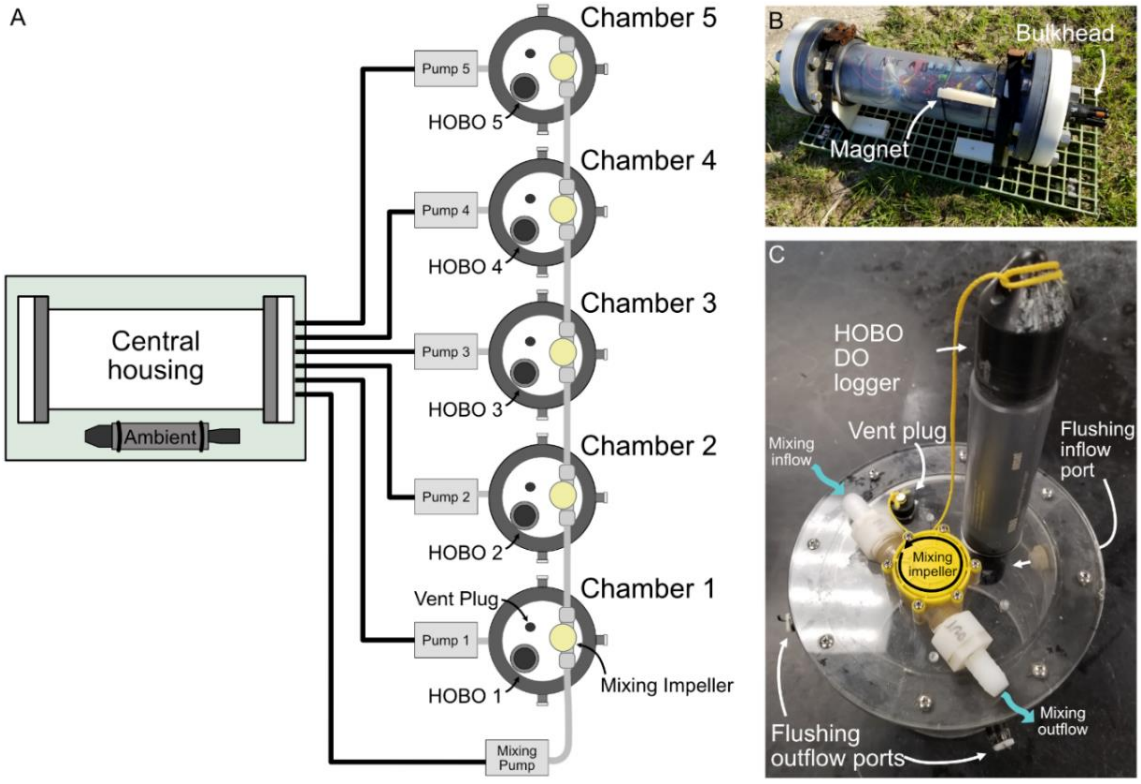

Figure 10. In-situ flow-through chamber system. (A) Central housing and chamber setup schematic diagram and photos of (B) the central housing and (C) one of the benthic chambers. The central housing contains the batteries and electronics and the pumps are controlled via connections through a wet-mate bulkhead. The HOBO taking the Ambient DO measurement is secured to the platform with the chamber housing. The housing is mounted to a rigid fiberglass platform for deployments. Once the housing and chambers are deployed and the pumps connected, the external magnet is moved into alignment with the internal magnetic switch to turn the system on. During a measurement period, the flushing pumps (pumps 1-5) sequentially turn on to flush the overlying water in the chambers, and then the mixing pump is intermittently turned on to agitate the overlying water of all the chambers to prevent stagnation.

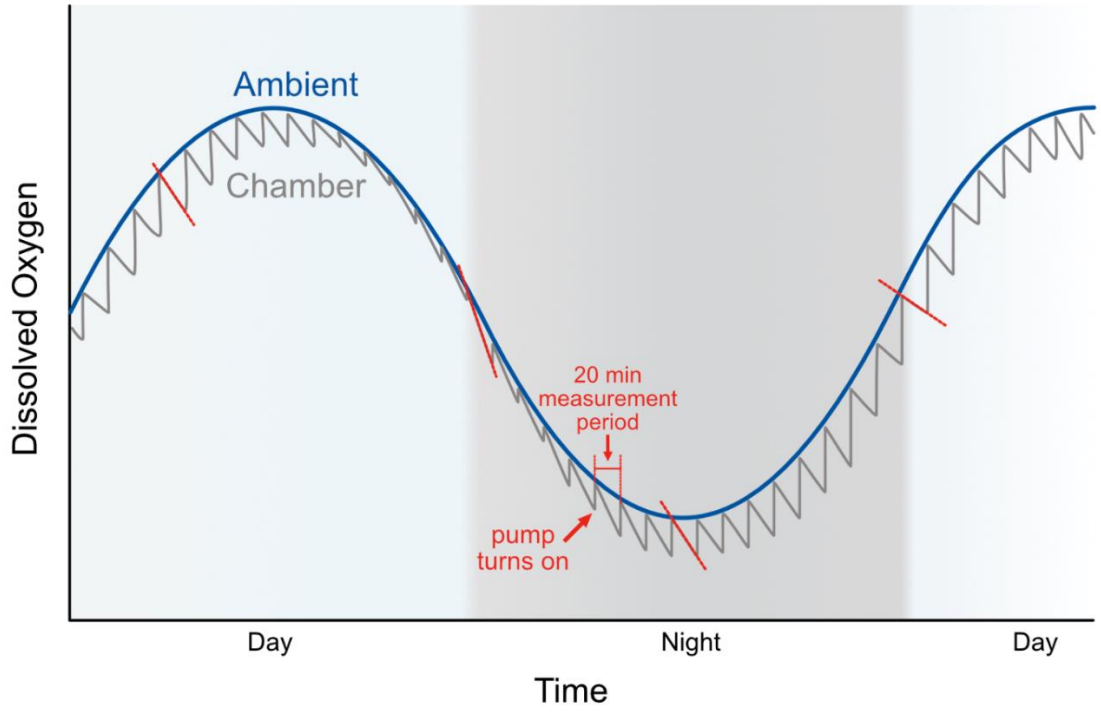

Figure 11. Schematic diagram of a diel oxygen cycle from the ambient DO measurement (blue line) and the "sawtooth" pattern from the DO in one of the benthic chambers (grey line). The grey shaded section of the plot indicates nighttime hours. Each measurement period is ~20 min. When the chamber pump is turned on, the overlying water is flushed with water of ambient DO concentration to start another measurement period. Slopes of the teeth can be compared at different times in the deployment to gauge change in SOD (red dashed line segments).

The central housing is constructed from 6-inch diam (15.24 cm) schedule 40 clear PVC tubing, capped on each end with a PVC-glued plastic flange, rubber gasket, and plastic endpiece which was secured with six ¾ x 10 X 3.5 long bolts and nuts (Table 4; Figure 10B). One endpiece has a SeaCon AWQ 4/24 6-port bulkhead mounted to connect the submersible pumps outside the housing to the electronics and power source inside the housing. The housing was seal-tested by deploying it at 20 m for ~48 hrs and we found no evidence of leaks after recovery. A 13.5V battery pack in the central housing powers the electronics and the pumps. The battery pack consists of three units connected in

parallel, with each unit having nine 1.5V D cell batteries connected in series. A spot welder was used to make the electrical connections between batteries and battery units and the entire battery pack was secured together with duct tape. Six SeaBird 5T/5P submersible 12V pumps were used for this build with the appropriate plug configuration to fit the bulkhead. An Arduino Uno microcontroller was used to control the pump cycling via 12V relays and recorded the start time of each measurement period with an Adafruit datalogging shield. Power to the device is cycled with a magnetic switch situated close to the housing wall so that the system can be turned on after the housing is sealed. When powered on, the Uno immediately begins executing the programmed code on a loop, with each loop representing a single measurement period. At the start of a loop, the Uno records the date and time and then sequentially turns each chamber Flush Pump on for 20 s to flush the overlying water in the chamber with water of ambient DO concentration. The code then executes 20 repetitions of turning the Mixing Pump on for 15 s and off for 45 s to mix the overlying water in the chambers and prevent stagnation. The loop then concludes and starts again. The duration of the measurement period (in minutes) is therefore determined by the number of times that the Uno is programmed to turn the Mixing Pump on and off. The annotated Arduino code can be found in Appendix A (Text A1).

Table 4. Materials and components list.

	Source	Notes
Central housing components		
6" Sched 40 clear PVC pipe	US Plastic	Item#: 34113
6" Sched 80 PVC socket companion flange (x2)	US Plastic	Item#: 28165
6" neoprene flange gasket (x2)	US Plastic	Item#: 28170
Endcaps (x2)	US Plastic	Item#: 45426 (custom-milled)
18-8 SS hex head screws	McMaster-Carr	Item#: 92186A851
316 SS hex nuts	McMaster-Carr	Item#: 97619A660
316 SS washers	McMaster-Carr	Item#: 90107A121
Arduino Uno Rev3 SMD	Arduino	Code: A000073
SD datalogging shield for arduino	Adafruit	Product ID: 1141
SD card	Amazon	Sandisk 32GB
12V FeatherWing power relay	Adafruit	Product ID: 3191
power and ground distribution blocks	Amazon	1/4" Stud Junction Bus bar Kits
Magnetic switch	McMaster-Carr	Item#: 8073A28
Terminal connectors	Amazon	strip blocks with spring clips
Bulkhead	SeaCon	AWQ 4/24 6-port
Submersible pumps	Seabird Scientific	SBE5P, PL, MCBH, STD VOLT, 3000 RPM, SLOW ST
Pump connector (x6)	tti	TTI Part Number: MC-S061-0060
Bulkhead connector (x6)	tti	TTI Part Number: AWQ-S011
Splice kits	Zoro	Zoro#: G2179484
Chamber components		
6" OD acrylic tubing (chamber body)	US Plastic	Item#: 44550
12mm cast acrylic sheet (chamber flange)	US Plastic	Item#: 44381 (custom-milled)
5.6mm extruded acrylic sheet (chamber top)	US Plastic	Item#: 44350 (custom-milled)
1/16" gasket material	McMaster-Carr	Item#: 8635K162
6-32 thread 316 SS truss head screws, 1" long	McMaster-Carr	Item#: 94792A717

Table 4 cont.

6-32 thread 316 SS serrated flange locknuts	McMaster-Carr	Item#: 91343A101
vent port plug	McMaster-Carr	Item#: 9545K115
Mixing impeller	Amazon	Water turbine generator retrofitted by removing the internal electronics and installing magnets in the impeller
Magnets	McMaster-Carr	Item#: 5862K143
Magnetic stirbar	McMaster-Carr	Item#: 5678K143
Mixing impeller hose barb fittings	McMaster-Carr	Item#: 5372K182
Outflow and inflow port fittings	McMaster-Carr	Item#: 5218K704
Outflow port locknuts	McMaster-Carr	Item#: 7877N103
HOBO DO logger	Onset	Part#: U26-001
1/2" ID rubber tubing	McMaster-Carr	Item#: 5233K68
Outflow caps	McMaster-Carr	Item#: 8546K12 (custom-made from nylon rod)

Five replicate benthic chambers were constructed. To construct a benthic chamber, an acrylic flange was glued to one end of a 6-inch ID clear acrylic tube, and a top cap secured in place with stainless steel screws (6-32) with a gasket between the flange and cap (Figure 10C). The top cap had a CNC-milled hole for attaching the HOBO dissolved oxygen logger and a smaller vent hole to allow for escape of any air bubbles and to vent water displaced during chamber deployment. Once deployed, a rubber stopper is placed in the vent hole opening to prevent water exchange. Screw holes were drilled in the top cap to mount the mixing impeller housing, and the magnetically coupled stirbar

suspended from the underside of the top cap beneath the impeller housing with a fishing swivel to allow it to rotate freely.

The chamber has one inflow and three outflow ports (½ inch diameter) for flushing the overlying water. The outflow ports are fitted with one-way valves constructed from negatively buoyant plastic caps threaded on a wire hooks. When the chamber is flushed the caps swing upwards and allow water to easily exit, and during the measurement period the caps cover the port openings to prevent backflow.

3.4 Assessment

3.4.1 Design concept and development

The setup was constructed through an iterative process of testing and troubleshooting and with the objective of potentially using the system in a variety of environments and at a range of water depths, which informed the rugged design of the central housing, the use of high depth-rated submersible pumps and the decision to mix chambers with pump-driven impellers. This resulted in a simplified design that can be expected to function similarly in dynamic, shallow subtidal waters and the deeper waters on the continental shelf.

Some researchers have noted that measurements acquired from benthic chambers tend to underestimate SOD compared to eddy correlation because the chamber structure restricts ambient flow, particularly in permeable sediments that experience flow-induced porewater flushing (Berg et al. 2013). Though this would be a valid critique of the use of benthic chambers in efforts to obtain maximally precise and accurate SOD

measurements, our objective in building this setup was to measure the effect of faunal activity throughout the diel cycle and enclosing some portion of the sediment was necessary to associate SOD directly with the resident fauna. Therefore, it is the relative difference between SOD in chambers with and without fauna that is informative rather than the absolute measurement of SOD.

3.4.2 Lab testing

We performed several operational tests on the chambers in the lab. To ensure that the chamber interior would be sufficiently enclosed, we performed leak tests in a laboratory flume system. A chamber was taken as a sediment core from the field, capped on the bottom, and brought back to the lab. The laboratory flume has a drop-down compartment for positioning objects level with the flume bottom. The compartment was covered in a piece of plastic sheet with a hole cut-out sized to hold the outside diameter of the test chamber. Inserting the test chamber into the plastic sheet resulted in the topmost core plane sitting 5cm proud of the plastic sheet surface. This replicated the positioning of the outflow ports on the cores relative to the benthos when deployed *in situ*. The chamber was then hooked up to the electronics and power and run as normal. Leakage was assessed by injecting colored dye through the top vent port, plugging the port, and observing for dye escaping during the incubation period. For this test, free stream flow speeds in the flume were measured using colored dye as ~4 cm s^{-1}. We observed no traces of dye escape during the incubation periods, and noted complete dye ejection during each flushing step, indicating both that the chamber overlying water is well contained during incubations and that the overlying water experiences complete exchange during flushing.

In early versions of the setup, each chamber had only one outflow port and was fitted with a low crack-pressure (1/3 psi) check valve to prevent backflow. This created issues during chamber flushing, as the check valve still provided enough resistance to flow that the chamber interior would pressurize and the chamber push up and out of the sediment, resulting in a failed deployment. To fix this issue, two more outflow ports were added and the check valve replaced with the plastic caps to allow for easy and unobstructed outflow during flushing. If these caps were to become stuck in the open position, exchange could occur between the chamber overlying water and the exterior water, corrupting SOD measurements. To assess the effect this may have on chamber SOD, we conducted an additional flume test. For this test, free stream flow speeds in the flume were increased to ~8 cm s^{-1} to maximize possible exchange. A chamber with sediment was positioned in the flume, similar to the previous leak test, and the system run with the chamber operating normally (i.e., with the outflow ports closed during the incubation period). After several incubation periods, the caps on all three outflow ports were then purposefully lodged in the open position and the system allowed to continue running. After several more incubation periods, the caps were dislodged and allowed to function normally again for the remainder of the trial (Figure 12A). SOD was not significantly different when ports were held open or functioning properly, though the p-value was very low (Figure 12B; one-way ANOVA, $p=0.0725$). This indicates that, though exchange may occur when the outflow ports are stuck open, this exchange is limited. It is also highly unlikely that all three outflow ports would malfunction simultaneously, so the likelihood of substantial leakage through the outflow ports was overall gauged to be low.

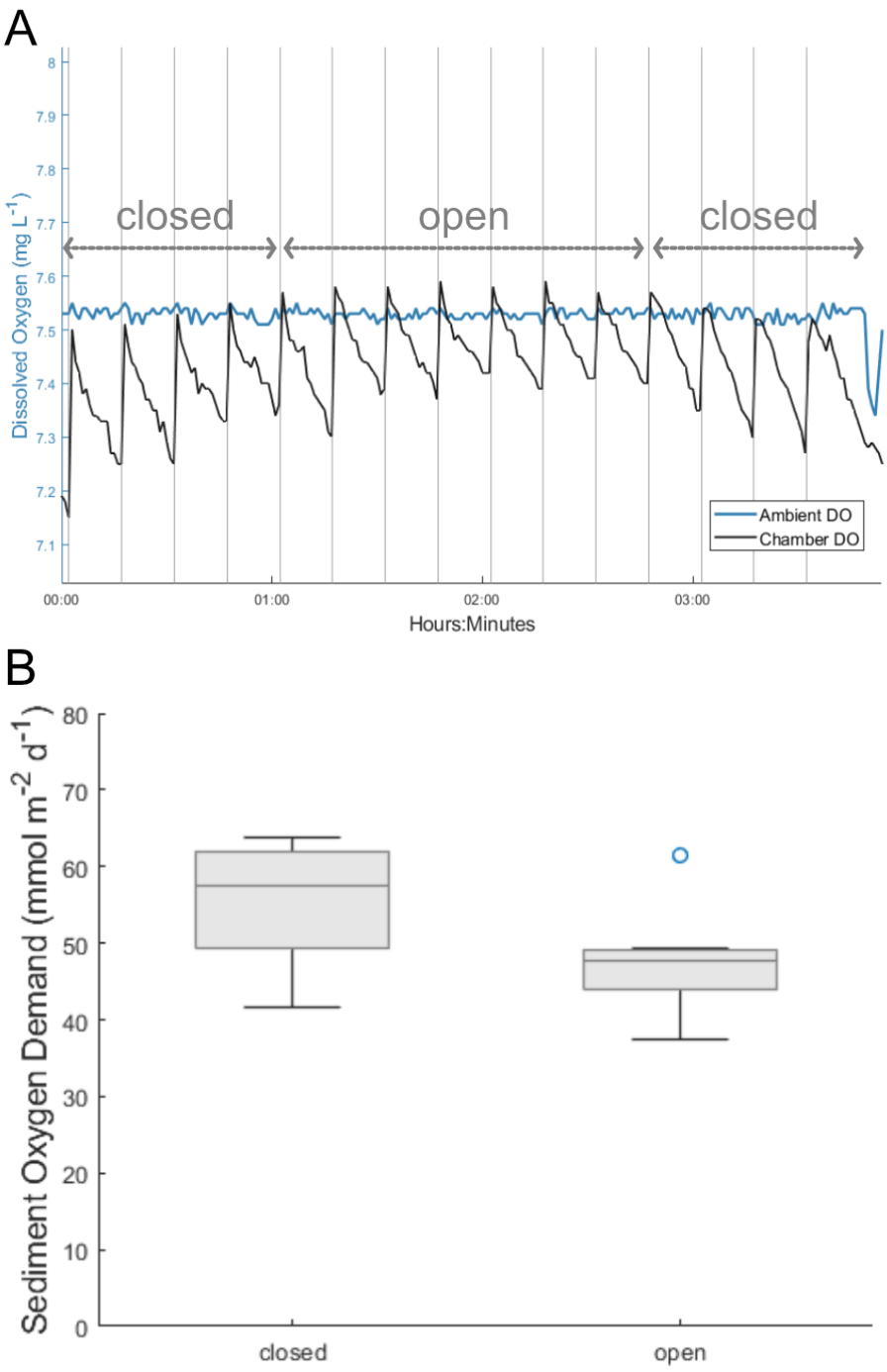

Figure 12. Results of leak test in laboratory flume for a benthic chamber with sediment. SOD was not statistically different during period of the test when ouflow ports were held in the open position compared to the period when the ports were operating normally, though the p-value was low (p=0.0725).

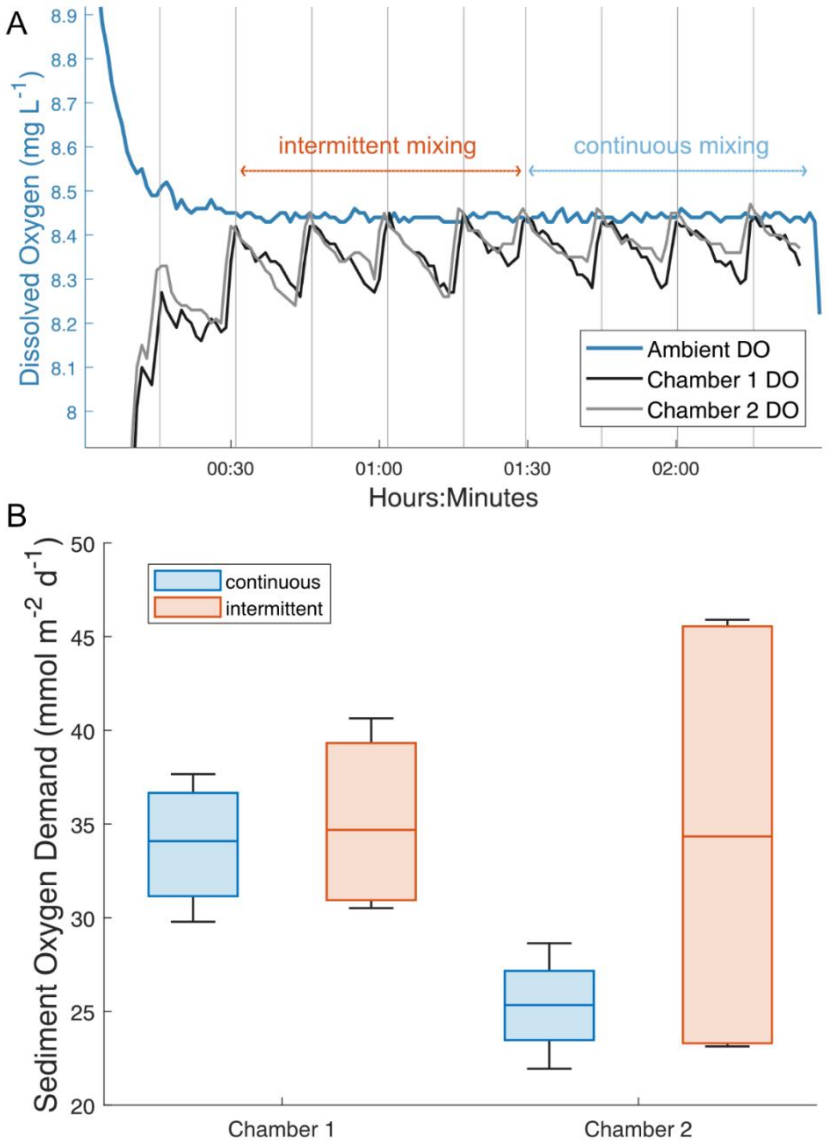

Figure 13. Results of mixing test in laboratory flume for two benthic chambers with sediment. The system was programmed to mix in cycles of 20s on:40s off for several measurement periods, and then the system was switched to mix continuously for several measurement periods (A). Vertical grey lines mark the beginning of each measurement period. There was no significant difference between SOD measurements when continuously mixing vs intermittently mixing for either chamber (B) ($p>0.05$).

In laboratory benthic metabolism chambers the overlying water is typically mixed continuously, however with *in situ* systems maintaining effective mixing can be a

challenge. A variety of mixing strategies have been used with *in situ* chambers, from battery-powered mechanisms mounted to the top of each chamber to paddle wheels that transfer ambient flow energy to the chamber interior (Tengberg et al. 1995). Because of the long deployment time of our *in situ* chambers, individual battery-powered stirring mechanisms were impractical, and paddle wheels would introduce problematic variability because of the inconsistency of ambient flow rates over time. The mixing apparatus for our system allows for simultaneous mixing of all the chamber using only one pump, and we set the system to mix the chambers intermittently instead of continuously to conserve battery power for the long deployment. To estimate the effect of intermittent mixing on SOD, we set up two sample chambers in a lab flume with the mixing apparatuses hooked up in series and ran the system for several measurement periods while intermittently and continuously mixing (Figure 13A). There was no significant difference between SOD when the chambers were being intermittently vs continuously mixed for either chamber (Figure 13B; one-way ANOVA, $p>0.05$), so for deployments the system was set to mix intermittently.

3.4.3 Field testing

The system was field tested in Gulf Shores, Alabama, USA, at a shallow (<1 m), sandy site in Bon Secour Bay, a partially enclosed embayment in southeast Mobile Bay (30.239478°, -87.894094°). All HOBO loggers were two-point calibrated the day before deployment. The central housing was secured to a fiberglass grid mesh platform (Figure 10B). An additional HOBO DO logger was mounted to the housing platform to measure the ambient DO concentration. The benthic chambers were deployed in a line at the bulkhead end of the housing, and the pumps attached to the inflow ports on each of the

chambers. The Mixing Pump was attached to a PVC pole embedded into the sediment so that the pump intake was suspended in the water column. Flexible PVC tubing (½ inch ID) was plumbed from the mixing pump outflow and connected in series between the mixing impellers on the tops of all the chambers. Prior to deployment, transparent surfaces of all the chambers were covered in duct tape to prevent photosynthesis inside the chambers during daylight hours.

The system was deployed from shore and recovered ~24 h later. At recovery, the chamber contents were sieved in the field through a 1mm mesh sieve and preserved in 70% EtOH with Rose Bengal to stain faunal tissue. Analysis of faunal communities in the chambers and their impact on SOD is described in Chapter IV. DO data were offloaded from each of the 5 chamber HOBO loggers and the ambient DO HOBO logger, plotted to observe the DO pattern throughout the diel cycle, and analyzed for SOD.

To properly test the system, we first had to confirm that (1) the ambient DO followed a diel cycle. The system was gauged to have operated successfully if, (2) the DO in the chambers exhibited the sawtooth pattern in relation to the ambient DO, (3) the chamber DO at each sawtooth peak matched the ambient DO at that time (indicating sufficient chamber flushing), and (4) SOD measurements could be collected throughout the diel cycle.

(1) Diel cycle

The ambient DO measured by the HOBO DO logger attached to the central housing platform roughly followed a diel cycle, with the maximum DO concentration of 12.95 mg L^{-1} at 5:25 PM and the minimum DO concentration of 3.42 mg L^{-1} at 1:34 AM (Figure 14).

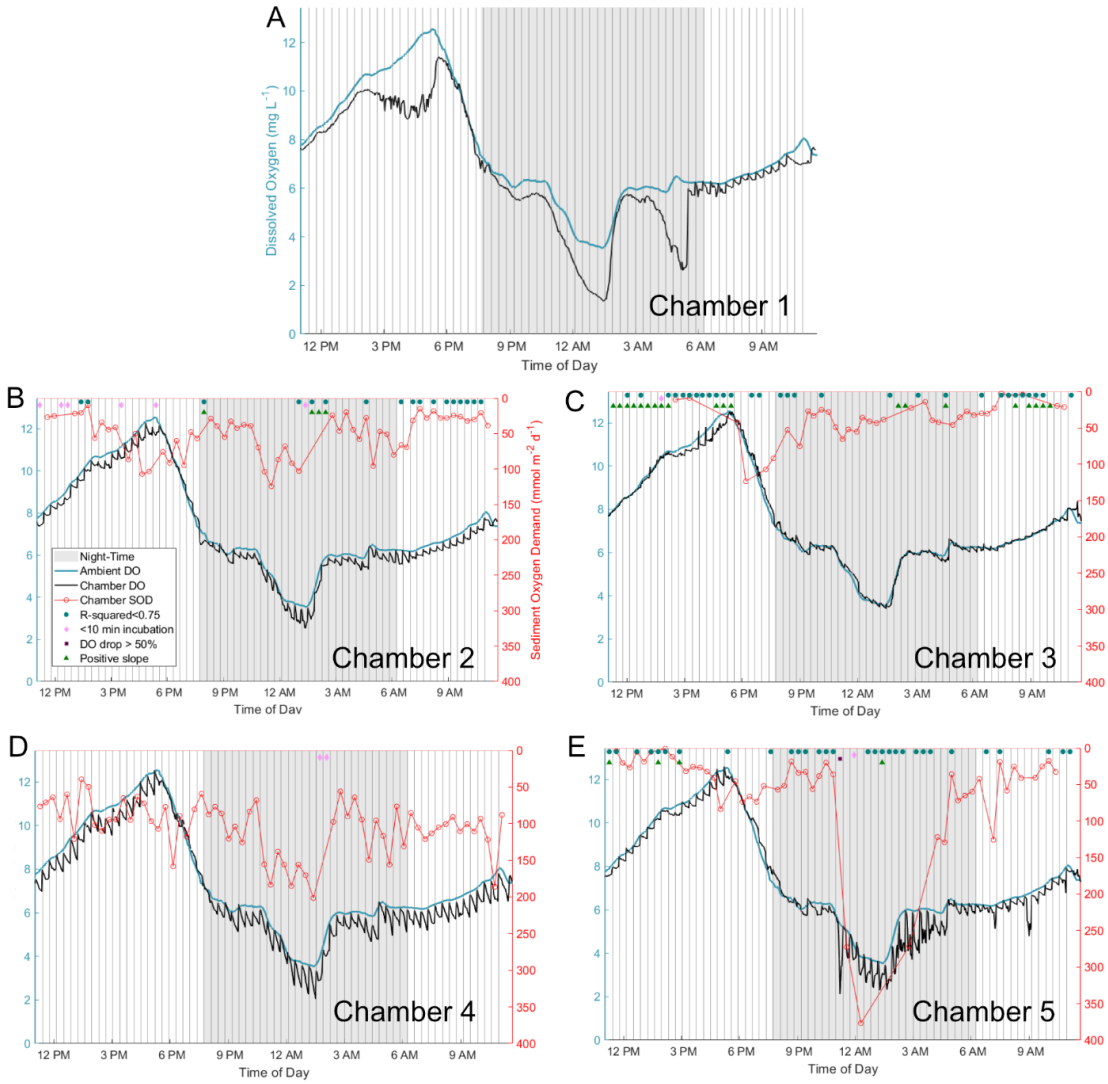

Figure 14. DO and SOD data from test deployment. Ambient DO (blue lines, data smoothed with 12-point moving average), chamber DO (black lines) and calculated SOD values (red points) from test deployment. Grey shaded areas are night-time hours, and vertical lines indicate timepoints when the overlying water was refreshed in the chambers, i.e., the beginning of each "measurement period". The chamber DO exhibits the desired "sawtooth" pattern in chambers 2-5. Chamber 1 appears to have malfunctioned for much of the deployment so was excluded from SOD analysis. SOD was calculated from the slopes of each of the measurement periods for chambers 2-5; measurements from slopes with regression fits (R^2) below 0.75 (blue circles), slopes that were calculated from incubations shorter than ten minutes (pink diamonds), and measurements that were taken during an incubation in which the DO in the chamber decreased by more than 50% of the starting DO (red squares) or had a positive slope (green triangles) were excluded. Measurements with both an SOD value and a blue circle are those that were flagged due to their low R^2 but included based on visual inspection.

(2) Sawtooth pattern

Chambers 2-5 show distinct sawtooth patterns with clear variations in the slope steepness between the different chambers (Figure 14). Chamber 1 appears to have malfunctioned for much of the deployment, likely due to the flushing pump working inconsistently, but started functioning properly at ~6 AM and continued until the deployment ended (Figure 14A). Because of this, we have excluded chamber 1 from further analysis, but note that the malfunctioning of the pump was clearly detectable from the data.

(3) Chamber flushing

To determine whether the chambers were being adequately flushed, the difference between the ambient DO and the chamber DO concentrations directly after the flush step of each measurement period (i.e., at the sawtooth "peaks") were plotted against the ambient DO concentrations for chambers 2-5 (Figure 15). Values close to zero indicate that the chamber DO was similar to the ambient DO after being flushed. The maximum deviation of the flushed chamber DO from the ambient was -0.54 mg L^{-1} (in chamber 4), and for every chamber at least 85% of chamber DO values after flushing were within ±0.25 mg L^{-1} of their corresponding ambient DO, indicating that the chambers were being sufficiently flushed throughout the deployment.

(4) SOD measurements

SOD was calculated from the linear slopes of the chamber "teeth" for all measurement periods in the deployment (Figure 14). Though many of our slopes were highly linear we also observed a variety of DO patterns within the incubations, ranging from irregular fluctuations to DO leveling off or drifting up near the end of the measurement period.

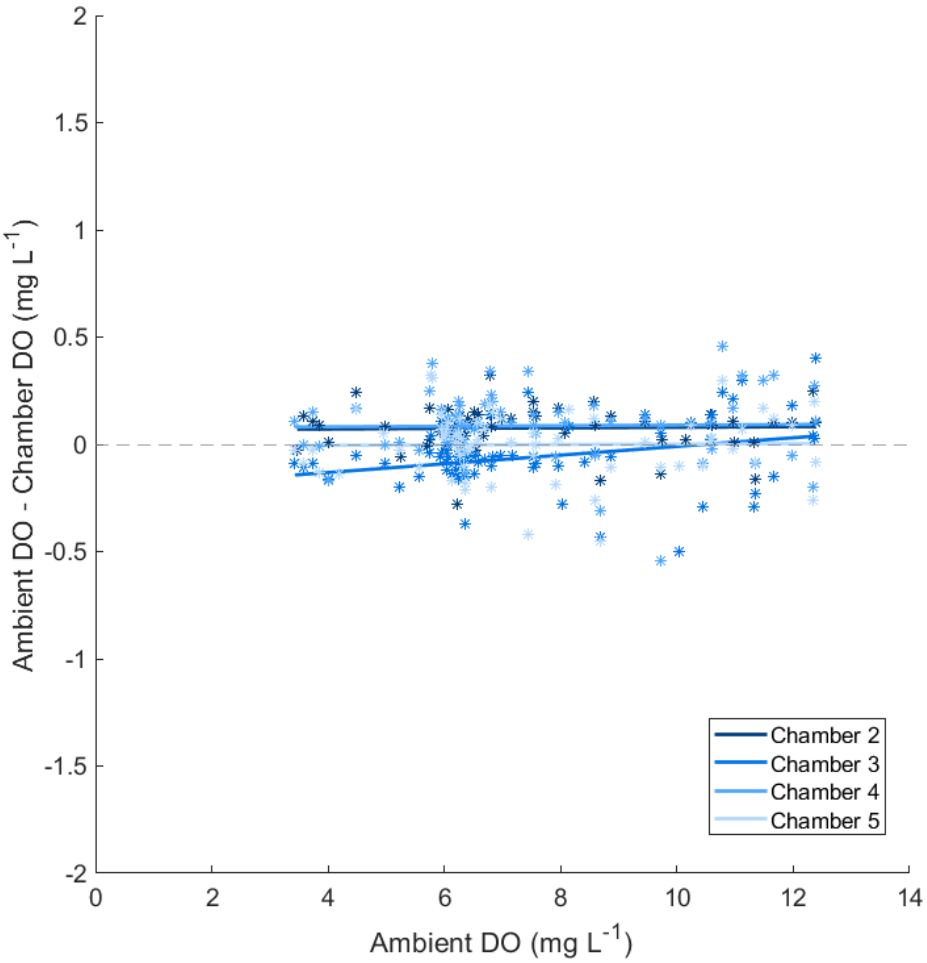

Figure 15. Matching of Chamber DO to ambient DO. Difference between the ambient DO and the simultaneous chamber DO directly after the flush step of each measurement period, plotted against the ambient DO at that time for chambers 2-5. The dotted line at y=0 indicates the chamber DO exactly matching the simultaneous ambient DO.

In cases where slopes did not appear linear for the entire incubation duration, slopes were calculated from a subset of the incubation data gauged to be linear. We then removed low quality or questionable SOD measurements from the data set based on certain criteria; we excluded measurements from slopes with regression fits (R^2) below 0.75, slopes calculated from incubations shorter than ten minutes (or less than half of the measurement period), and measurements taken during incubations in which DO in the

chamber decreased by more than 50% of the starting DO or had a positive slope (Figure 14). Summary data for the SOD measurements is presented in Table 5.

Table 5. Chamber SOD measurements.

Chamber #	Number of Measurements	Mean SOD ± Std Dev (mmol m^{-2} d^{-1})
2	57	51.4 (± 28.6)
3	36	39.0 (± 27.0)
4	65	104.9 (± 36.0)
5	47	60.0 (± 72.6)

Excluding measurements based on R^2 value could severely bias the data because regressions with shallower slopes tend to have lower R^2 values than steeper-sloped regressions, given the same variability. This means that incubations with very low SOD ("flat" DO trends through time) would be disproportionately discarded even though they may reflect real patterns in the data. To account for this, all incubations that were flagged as having R^2 values lower than the 0.75 threshold were visually inspected, and those that were highly linear but with a flat trend through time added back into the data set, while those with irregular trends discarded.

3.5 Discussion

SOD is a challenging parameter to measure, particularly in the field, and the existing methods to do so are limited in either the temporal or spatial resolution they offer. Using this benthic chamber setup we were able to generate repeated measurements of SOD throughout the diel cycle in connection with discrete areas of sediment. Filtering

the data by quality criteria and visual inspection of trends yielded a data set of high-quality linear slopes, and these SOD measurements fell within the range expected from other studies conducted in similar habitats using benthic chambers (Table 2 in Huettel et al. 2014; Table 5). Berg et al. (2013) reported nighttime SOD rates ranging from 50 to 120 mmol m^{-2} d^{-1} from benthic chambers deployed in permeable river sediments at a similar latitude to our test site, and the majority of SOD values collected from our setup fit comfortably in that range (Berg et al. 2013).

Filtering the data based on the stated quality criteria resulted in different numbers of useable measurement periods depending on the chamber, with a greater number of high-quality measurements generally produced in chambers with higher average SOD (Table 5). Chamber 5 is the exception; SOD increased dramatically in the nightly low DO period and DO in many of its incubations during that period followed a highly irregular pattern (and therefore excluded them from analysis) (Figure 14E). We suspect that faunal activity may account both for the period of much greater SOD and for the irregular DO patterns, and this subject is discussed further in Chapter IV. There was also considerable variability between chambers and even between successive SOD measurements within a given chamber, however such variation is typical. Data from eddy correlation studies have indicated that SOD can vary widely on short timescales (on the order of minutes), a phenomenon also demonstrated in our measurements (Berg and Huettel 2008; Berg et al. 2013). Furthermore, in our setup the average SOD varied substantially between chambers (Table 5, Figure 14), suggesting variation on small spatial scales that may be driven by faunal activity.

3.6 Comments and Recommendations

3.6.1 System construction

Our objective in building this system was to demonstrate the utility and practicability of the semi-flow-through chamber concept, and we would advise those wishing to build a similar system to tailor it for their specific application. Several components in our setup were used because they were easy to access or already in our possession, however depending on the application a more economical version of some components would do as well or better. For example, the flushing and mixing pumps used in our system are depth rated to 600m, however if the system will be used only in very shallow water we would advise using simple aquarium pumps and modifying the power connector with a wet-mate plug into the bulkhead. The system could likewise be scaled up or down depending on power requirements and logistical restrictions of deployment. Other aspects of the setup, such as the construction of the chamber outflow ports, provided the most workable solution during development but could be further optimized in a new version, and we would encourage those intending to build their own system to experiment with alternatives.

3.6.2 System settings and deployment considerations

The Arduino code controlling the execution of the system has three major features that may be changed to adjust operation: the measurement period length, the flush duration, and the mixing settings.

The measurement period length is set by changing the number of iterations that the Mixing Pump is turned on or off and will control the duration of each “sawtooth”.

Selecting a measurement period length requires striking the correct balance between collecting sufficient data for slope calculation and avoiding an excessive drop in DO. Because SOD is positively correlated with DO concentration (Burdige 2006), long incubations risk the chamber DO decreasing to the point of changing the SOD slope, resulting in a non-linear pattern. However, short incubations may not provide enough time for a consistent pattern to appear. Additionally, the measurement period selected must take into consideration how SOD may change throughout the diel cycle and allow for slopes to be calculated at SOD extremes. Selecting an appropriate measurement period will require some trial and error, and we recommend testing several measurement period lengths to determine the optimal settings.

The flush duration is set by changing the amount of time each chamber Flush Pump is turned on at the beginning of each measurement period. There is little risk of over-flushing, however under-flushing may result in incomplete exchange of the chamber overlying water. This would be noticeable as several successive sawtooth peaks not matching with the ambient DO at the start of each measurement period. The pumps used in our setup were set to pump ~100 mL s^{-1} and the overlying volume of the chambers was ~1 L, so pumps were left on for 20 s each, or twice the amount of time needed to flush the chambers assuming perfect replacement of water. Our test deployment took place in sandy sediments regularly exposed to high wave action, so disturbance of sediment within the chamber from flushing was of low concern. However, in finer-grained, muddier, consolidated sediments the pump rate should be slowed to prevent chamber flushing from eroding the sediment. This could be done by directly restricting the intake of water for each chamber Flush Pump, i.e. by covering with screen mesh or attaching an

adapter with a smaller diameter opening, or by branching the tubing from a single pump to multiple chambers therefore decreasing flow rate to each chamber. Note that with a decreased flow rate the flush time will have to be increased to ensure sufficient chamber flushing.

The mixing conditions can be set by changing the amount of time the Mixing Pump is turned on versus off during each loop, and the amount of mixing time necessary may vary depending on the pump and the mixing apparatus in the chamber. Our Mixing Pump had a high flow rate and power draw, so we turned them on intermittently to avoid over-mixing the chambers in addition to conserving battery power. In setups using Mixing Pumps with lower flow rates and power draws, we recommend increasing the amount of time spent mixing as much as possible.

CHAPTER IV EFFECTS OF DIEL OXYGEN CYCLING AND BENTHIC MACROFAUNA ON SEDIMENT OXYGEN DEMAND

4.1 Abstract

Shallow marine soft sediments serve an important ecological function by respiring organic matter, which consumes dissolved oxygen (DO). Sediment oxygen demand (SOD) depends on overlying water DO concentration but can also be altered by mixing and irrigating activities of sediment macroinfauna. Shallow coastal oxygen patterns can vary substantially on short time scales, frequently following a diel cycle caused by photosynthesis increasing oxygen during the day and respiration consuming oxygen at night. In this study, we examined how SOD varied over a diel cycle with increased presence of macroinfauna. We constructed and deployed in situ flow-through benthic metabolism chambers to measure SOD at a high temporal resolution in discrete sediment patches. We found that sediments with more macroinfauna had greater average SOD over the diel cycle, consistent with previous studies. Interestingly, we found an interaction between the effects of faunal biomass and DO on SOD, suggesting that macroinfauna increase their activity in response to the nightly low oxygen, presumably by enhancing irrigation. SOD was also highly variable on a sub-diel timescale, and more variable in sediments with more macroinfauna. This indicates that sediment oxygen demand is dynamic and highly sensitive both temporally, on very short timescales, and spatially, in terms of resident fauna. High temporal and spatial resolution measurements, particularly on the diel scale, are critical to accurately estimate sediment metabolism.

4.2 Introduction

Benthic macroinfauna can significantly enhance sediment oxygen demand (SOD) by mixing or pumping water through the sediment (Aller 1978; Norling et al. 2007). This function is often lost when dissolved oxygen (DO) conditions in the overlying water decline, driving faunal mortality and typically lower SOD (Diaz and Rosenberg 1995; Middelburg and Levin 2009; Sturdivant et al. 2012). The effects of persistent low DO on sediment communities have been well studied, however in shallow, productive coastal environments DO can vary dramatically on short timescales (Wenner et al. 2004), following a diel cycle with high DO concentrations during peak light periods due to high photosynthesis rates and low, often hypoxic (DO < 2 mg L^{-1}) concentrations at night driven by respiration (Tyler et al. 2009).

Though there has been extensive research on the effect of prolonged hypoxia on both sediment geochemistry and infaunal communities (Diaz and Rosenberg 1995; Rosenberg et al. 2001; Middelburg and Levin 2009; Seitz et al. 2009; Lehrter et al. 2012; Gammal et al. 2017), few studies have examined sediment response on a diel scale. One study on diel changes in benthic metabolism in coral reef sediments found a positive relationship between DO concentration and SOD, with a 2.8-fold increase in flux between minimum and maximum DO (Clavier et al. 2008). It has recently become possible to measure sediment flux with a high temporal resolution using the eddy correlation technique (Berg and Huettel 2008), and oxygen fluxes in shallow, permeable sediments were revealed to have high variability between daytime and nighttime fluxes but also between successive measurements, taken on timescales of minutes to hours

(Berg et al. 2013). However, studies with high frequency SOD measurements remain sparse.

A 2004 study by Wenzhofer and Glud is the only known investigation into the relationship between diel changes in sediment faunal behavior and changes in sediment oxygen demand. They measured sediment-water oxygen exchange rates with a benthic chamber, microprofiled the sediment, and observed temporal and spatial variability of sediment oxygen distribution with planar optodes to characterize diel patterns in SOD (Wenzhöfer and Glud 2004). They observed increased sediment oxygen uptake in benthic chambers at the onset of darkness which diminished throughout the night, in contrast to only minor diel changes in oxygen microprofiles. This difference, as well as diurnally fluctuating oxygen concentrations around faunal burrows, led the authors to attribute the changes in oxygen flux in part to the diel rhythms of faunal activities. In this study, oxygen concentrations were fairly constant across the diel cycle, thus DO patterns were not driving these behavioral patterns.

Faunal response to declining DO can be complex and their activity may not necessarily change directly with DO concentration. When DO is low but not lethal, many taxa will maintain or even increase their activity to manage the induced stress (Diaz and Rosenberg 1995; Riedel et al. 2014). For example, Gurr et al (2018) found that the cardiac activity of the Atlantic bay scallop *Argopecten irradians* varied inversely with diel-cycling hypoxia, and that at moderately low DO (< 5 mg O_2 L^{-1}) the scallop maintained its heart rate independent of DO concentration, but below 2 mg O_2 L^{-1} heart rate declined severely (Gurr et al. 2018). Infauna inhabiting sediments in shallow, productive waters where diel oxygen cycling occurs are likely acclimated to variability in

oxygen availability, and particularly to short but repeating bouts of low DO, and may compensate by altering their irrigation, burrowing and feeding activity to affect sediment oxygen consumption over the day/night cycle. However, this variability remains largely undescribed since it is difficult to capture with existing methodologies.

In this study we examined how diel-varying oxygen concentrations and the presence of benthic macrofauna affect SOD throughout a diel cycle using a custom-built benthic chamber system to capture both temporal and spatial variability. We expected (H_1) that sediments with more infauna would have greater SOD overall than less populated sediments. Further, we hypothesized that infauna would alter the relationship between DO and SOD, either (H_{2A}) that infauna would decrease their activity levels when oxygen was low, and this would result in a stronger positive relationship between DO and SOD, or (H_{2B}) that infauna would irrigate their burrows more during the low-oxygen period of the diel cycle, increasing SOD at low DO and flattening the relationship between DO and SOD. We also expected (H_3) that the presence of infauna would contribute to greater sub-diel variability in SOD, i.e., variability on the scale of minutes to hours, as behaviors can change on short time scales.

4.3 Materials

4.3.1 Experimental design

We measured SOD in a shallow, sandy site in Bon Secour Bay, Mobile Bay, AL, (30.239478°, -87.894094°), using custom-built *in situ* semi-flow-through metabolism chambers (Chapter III) The site was subtidal (<1 m depth) and easily accessible from

shore. Previous sampling at the site indicated a patchy community of infauna, with large areas of sparsely populated sand dotted with tubes of the polychaete worm *Diopatra cuprea*. The chamber setup consists of a central housing containing battery power and the electronics of the system, and five replicate benthic chambers (Figure 10). The central housing controls and powers submersible pumps that are each attached to one of the chambers, as well as a pump that mixes the overlying water in the chambers. When the system is deployed, the chambers are periodically flushed with water from the external environment and then allowed to incubate for a short time before being flushed again. This results in a sawtooth pattern in the DO concentrations within the chambers through time, with each tooth being a replicate incubation, and the slopes of these incubations can be used to calculate SOD repeatedly throughout the diel cycle and in association with a discrete area of sediment and the fauna within.

The chamber system was deployed near midday and recovered the following day in three ~24 hr deployments (7-8, 10-11 and 11-12 August 2021). Care was taken when deploying the chambers to sample both in bare sand and areas with worm tubes visibly protruding from the sediment. The chambers were shaded to prevent photosynthesis in the daytime, and were flushed at 20 min intervals for the duration of the deployments. After each deployment, the contents of each of the chambers were sieved through a 1 mm mesh sieve in the field and preserved in 70% ethanol with Rose Bengal stain. Preserved samples were then sorted and infauna identified to lowest practical taxonomic level and counted. Shannon-Weiner Diversity index was calculated for each sample using PRIMER-e statistical software (Clarke and Gorley 2015). Total wet biomass of all fauna was measured for each chamber sample as well as total biomass of each of the most

dominant taxa. Because it is reasonable to assume that SOD scales with biomass, we used faunal biomass as the metric for faunal presence in subsequent analyses.

Sediment from the study site was analyzed for sediment geochemical properties. Three 10-cm diameter sediment cores were taken in the field, vertically sectioned in 1 cm increments, and stored at -20 ºC until processing. Porosity was calculated from the conversion equation in Jackson and Richardson (2007) using weight lost after drying at 70 ºC for >24 h (Jackson and Richardson 2007), and percent organic matter content was calculated as loss-on-ignition after burning at 500 ºC for 6 h. Measurements were averaged for each sectioned depth across the three sediment cores.

4.3.2 SOD calculation and analysis

SOD was calculated from the slope of the linear regression for the replicate incubations with a custom Matlab script (The MathWorks Inc. 2021). Though many of the slopes were linear, some displayed an irregular pattern and were not useable. We removed low-quality data according to the criteria outlined in Chapter III; SOD calculated from slopes with R^2 values below 0.75 (unless determined to be linear by visual inspection), slopes calculated from incubations shorter than 10 minutes, and measurements taken during incubations in which DO in the chamber decreased by more than 50% of the starting DO or had a positive slope were removed from the data set. One of the chamber flushing pumps also repeatedly malfunctioned in all three deployments, so data from that chamber were excluded from the analysis. This resulted in n=4 per deployment, or n=12 total.

The effect of faunal presence on SOD throughout the diel cycle (H_1) was assessed by performing linear regressions on all measurements of SOD, with faunal biomass and

DO as predictors. The relative effect of fauna on SOD in the high vs low DO periods of the diel cycle (H_2) was assessed through multiple linear regression of SOD as a function of DO and faunal biomass, specifically examining the interaction term. Evaluating sub-diel variability in SOD was challenging because SOD was predicted to depend on DO, which varied over time. There were also numerous missing data points because not all chamber runs had usable slopes for every measurement period. To address these problems, we conducted a smoothing analysis. After detrending the SOD data for each sample using the sample mean, we used a weighted moving average to fit a smoothing curve to the time series of each sample's SOD measurements. This analysis was performed iteratively on each sample's SOD data using increasing numbers of adjacent points for the moving average (hereafter "span size") to the data (Appendix B, Figure B1). Smoothed fits were generated for odd numbered span sizes from 1 to 29 points. 29 was selected as the maximum span size because all samples approached an asymptote at relatively small span sizes so calculations at greater spans was deemed unnecessary. We then calculated the residual sum of squares (RSS) of the smoothed fit at each span size and examined the change in RSS with increasing span size. If the SOD data contained high sub-diel variability, we expected a steep initial increase in RSS at small span sizes and a flat trend to emerge as span size increased. If infauna increase sub-diel variability, samples with more infauna would be expected to have a steeper initial slope. All analyses were performed in Matlab R2021a using custom script.

4.4 Results

The ambient DO followed a diel cycle in all three deployments (Figure 16). Both the maximum DO concentration and the time of day of maximum DO varied between deployments. The minimum DO concentration was similar among the three deployments (~3.4 mg L^{-1}), however it occurred at different times in the nightly low DO period. Deployment 1 displayed an irregular pattern during the night-time hours, with a sudden, brief dip in DO beginning around 12 AM. Temperature data from the HOBO logger displayed a concurrent bump in temperature at this time (Appendix B, Figure B2), indicating that this may be the result of a water mass moving through the area.

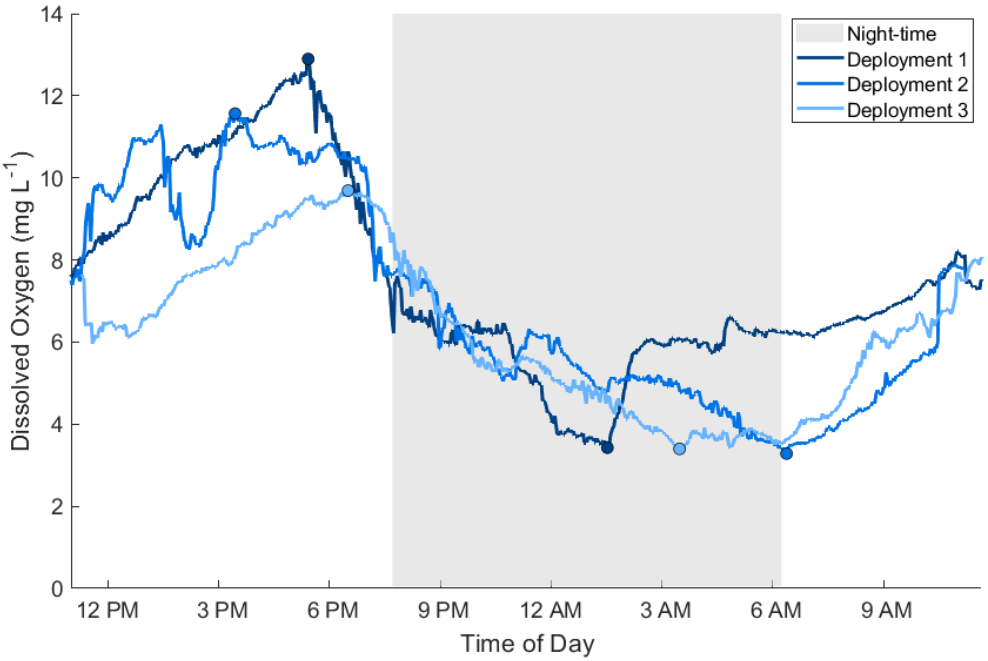

Figure 16. Ambient oxygen patterns for the three deployments. The shaded box indicates approximate night-time hours (sunrise and sunset times did not differ more than 5 minutes across deployments). Colored dots mark the maximum and minimum DO concentrations for each deployment.

Infaunal community abundance was dominated by mobile subsurface deposit feeders in the polychaete families Nereididae, Capitellidae and Orbiniidae, and by corophiid amphipods (Figure 17A). Total faunal wet biomass ranged from 0.45-8.03 g m^{-2}, with both the maximum and minimum values found in samples from deployment 1 (Figure 17B). Biomass was dominated by Orbiniid and Nereid worms.

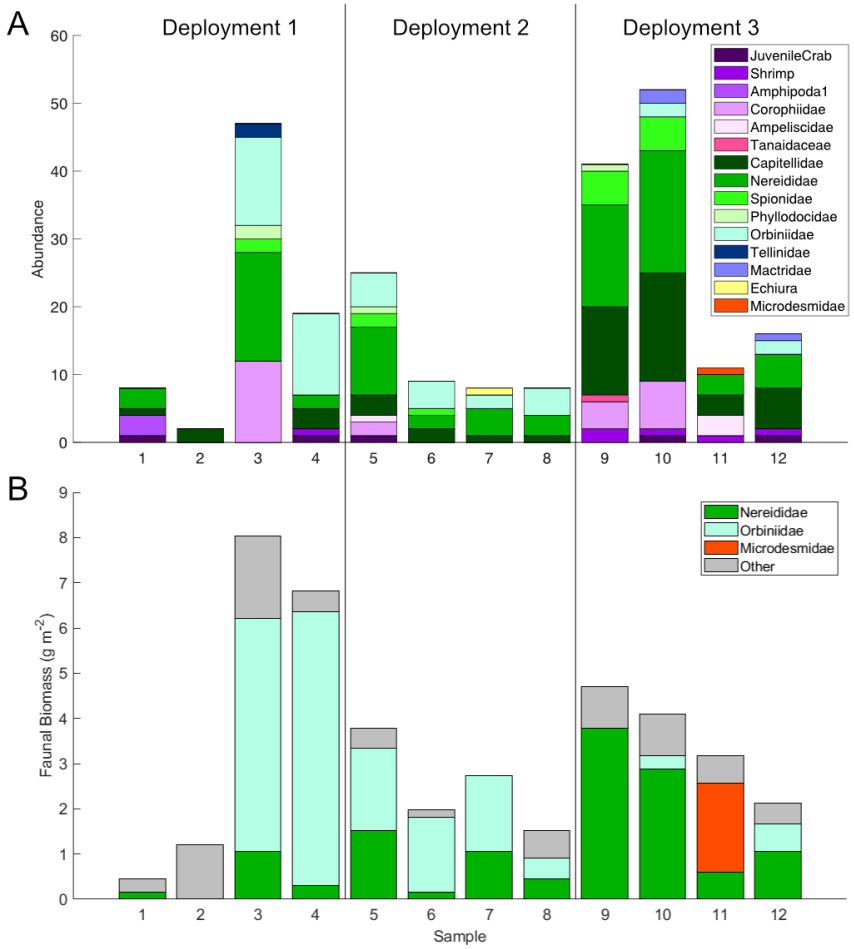

Figure 17. Macrofaunal community data. (A) Faunal community composition by abundance and (B) faunal wet biomass by highest contributing taxa. Abundances were dominated by the polychaete families Nereididae, Capitellidae, and Orbiniidae, and by Corophiid amphipods. Orbiniids and Nereids contributed most of the biomass in most samples, though in deployment 3, sample 11 contained a single burrowing wormfish (Microdesmidae) that made up the majority of biomass of that sample.

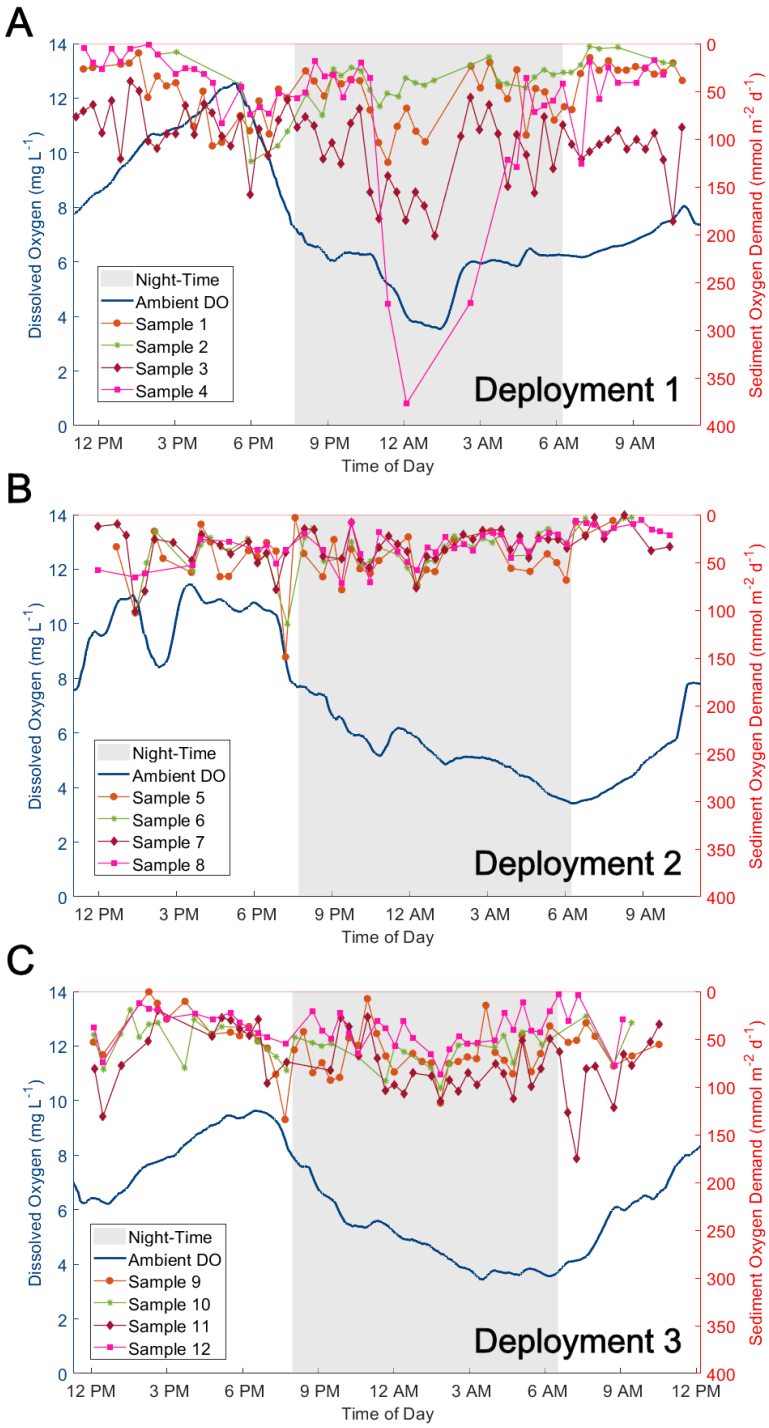

Figure 18. Ambient DO and calculated SOD values throughout the three deployments (A-C). Note that the axes for sediment oxygen demand are inverted. The Ambient DO data have been smoothed using a moving average with a window size of 12 to increase readability.

One of the chambers in the third deployment (Figure 17, sample 11) had relatively low faunal abundance but contained a large burrowing wormfish (Microdesmidae) that contributed 62% of the biomass of that sample. We did not find any *D. cuprea* in the samples despite seeing their tubes when deploying the chambers and finding their tube caps in the preserved samples. However, *D. cuprea* can extend their tubes up to 1 m deep into the sediment (Woodin 1978), and we suspect that some may have been enclosed in the chambers but evaded collection by retreating deeper into the sediment than the chamber was able to sample.

The average porosity of all depths was 38%. Porosity was slightly higher in surface sediments but remained consistent with increasing depth (Appendix B, Figure B3A). Organic matter content was consistently very low at all depths, with an average of 0.22% (Appendix B, Figure B3B).

Table 6. Summary data of SOD measurements and faunal community.

	Sample	n	Mean SOD ± Std Dev (mmol m^{-2} d^{-1})	Species Richness	Total Abundance	Biomass (g m^{-2})	Shannon-Weiner Diversity
Deployment 1	1	57	51.2 (±28.6)	4	8	0.45	1.255
	2	36	39.0 (±26.9)	2	3	1.21	0.636
	3	65	104.9 (±36.0)	6	47	8.03	1.474
	4	47	60.0 (±72.6)	5	19	6.82	1.129
Deployment 2	5	38	45.9 (±28.1)	8	25	3.79	1.733
	6	42	36.6 (±22.9)	4	9	1.97	1.273
	7	49	34.1 (±19.8)	4	8	2.73	1.213
	8	46	31.8 (±17.5)	3	8	1.52	0.974
Deployment 3	9	49	59.2 (±26.5)	7	41	4.70	1.544
	10	39	55.7 (±19.1)	8	52	4.09	1.628
	11	46	75.5 (±33.0)	5	11	3.18	1.499
	12	43	38.9 (±19.2)	6	16	2.12	1.511

SOD patterns throughout the diel cycle are shown for each sample in the three deployments in Figure 18. The greatest individual measures of SOD were by far in samples 3 and 4 in deployment 1, which also had the greatest faunal biomass among all samples (Table 6). The highest SOD also occurred during the short dip in DO concentrations during that deployment. Deployment 2 displayed comparatively low SOD among all four samples (Table 6, Figure 18B), while deployment 3 measures were moderately higher (Table 6, Figure 18C).

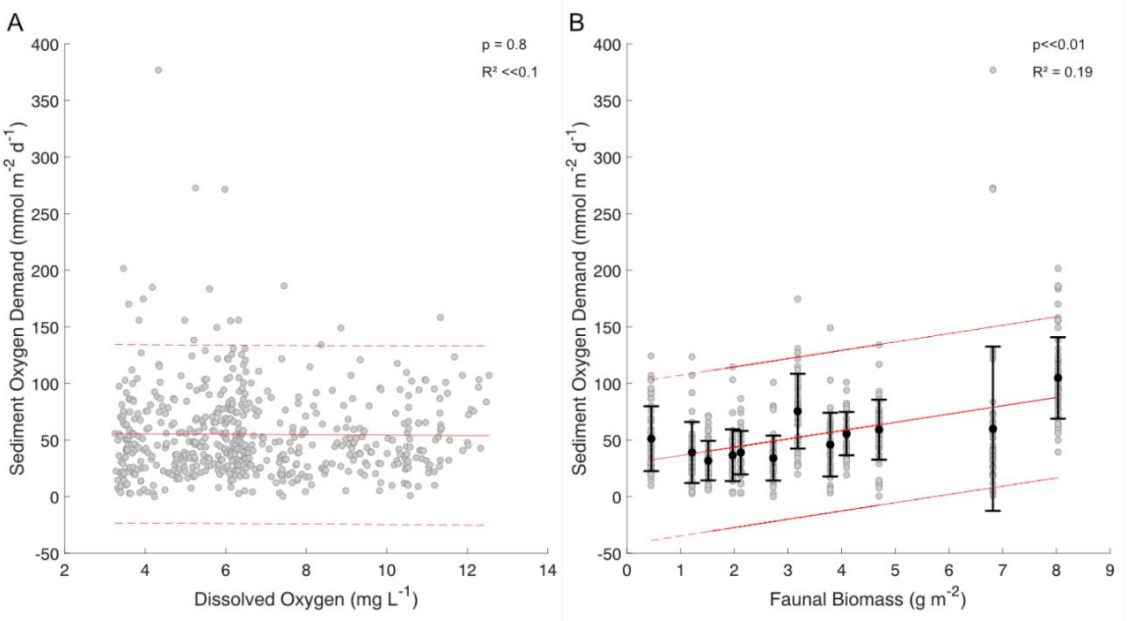

Figure 19. Regressions of SOD with (A) DO, and (B) faunal biomass. Individual SOD measurements are shown in grey points. Solid red lines depict the linear model, with dotted red lines as 95% confidence bounds. The faunal biomass plot also contains estimates of the mean and standard deviation of SOD for each sample, shown as black points and bars.

A simple linear regression indicated no dependence of SOD on DO (p=0.8; Figure 19A), however a regression with biomass revealed a significant relationship (p<<0.001,

R^2=0.19; Figure 19B). The multiple regression with both DO and faunal biomass showed a significant interaction in effect on SOD ($p<<0.001$), with a slightly improved model fit (R^2=0.25) from the model containing only faunal biomass. To understand this interaction, we performed linear regressions of DO and SOD for each sample (Appendix B, Figure B4) and regressed the resulting slopes against faunal biomass (Figure 20A).

This analysis was performed to determine if faunal biomass significantly affected how SOD varied with DO throughout the diel cycle. We found a significant negative correlation ($p=0.0047$), with SOD increasing with increasing DO at low faunal biomass (Figure 20B) but decreasing with increasing DO when faunal biomass was high (Figure 20C).

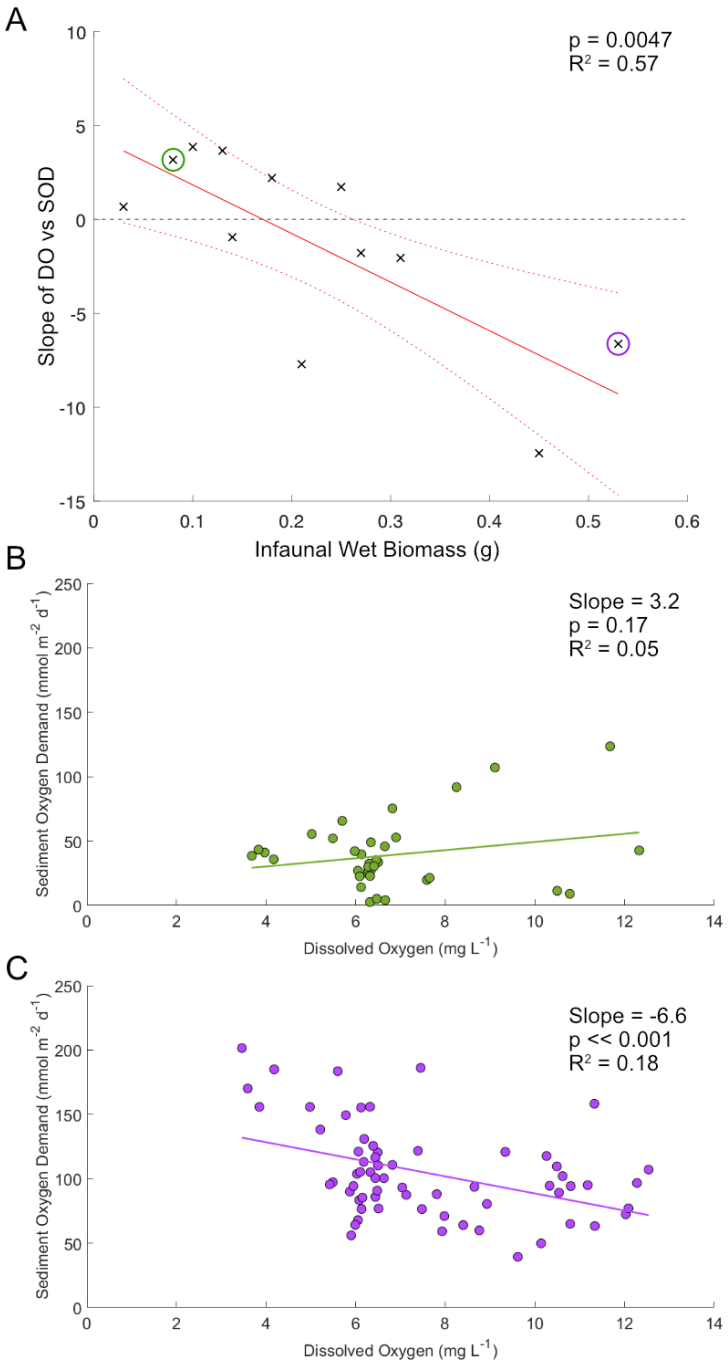

Figure 20. Regression of the slopes of DO vs SOD against faunal biomass. (A) Solid red line is the regression, and dotted red lines are 95% confidence bounds. The dotted line at zero indicates where SOD shows no dependence on DO. Circled are examples of slopes from a low biomass sample in green (sample 2) and high biomass sample in purple (sample 3), with the DO vs SOD regressions for those samples shown in (B) and (C), respectively. Note that the slope of the regression in the low biomass sample is positive, while the slope is negative in the high biomass sample.

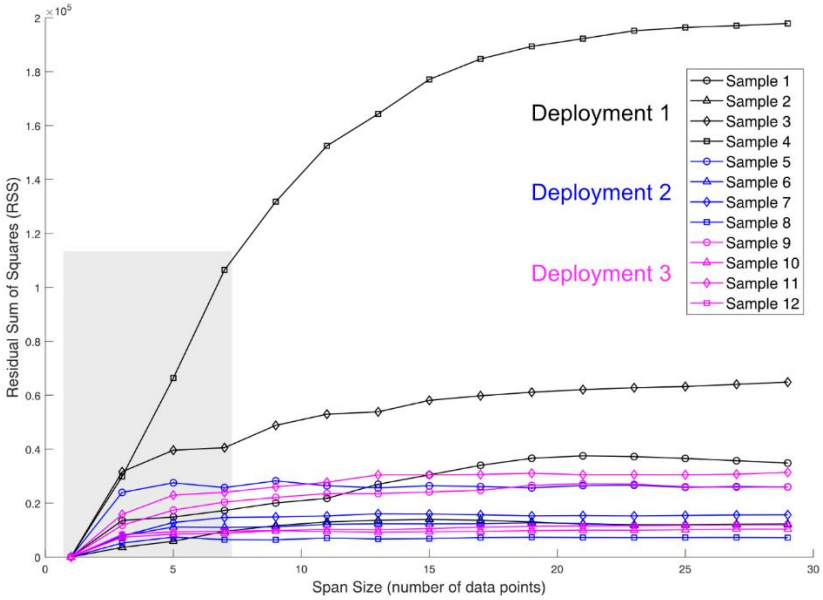

Figure 21. Residual sum of squares (RSS) for smoothing fits performed with moving averages of an increasing number of points (span sizes).

We observed high variability in SOD measurements between and within samples (Figure 18). In most samples the RSS steeply increased as span size widened, showing an immediate large RSS increase even when the span is widened from one to three adjacent points, and approached an asymptote as the span size increased (Figure 21). In all samples RSS increased to greater than 50% of the sample's maximum as span size increased to 7 points (grey box in Figure 21). The linear initial slopes for each sample (a metric of high-frequency variability) were regressed against faunal biomass and revealed a significant relationship (Figure 22).

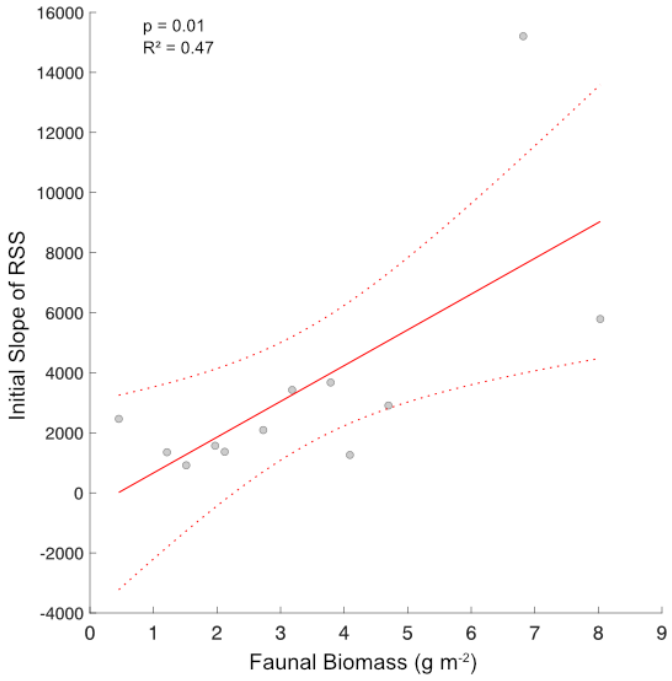

Figure 22. Regression of initial slopes of RSS values against faunal biomass.

4.5 Discussion

Overall, SOD was greater in sediments with more fauna (H_1) (Figure 19B), consistent with previous studies (Aller 1988; Pelegri and Blackburn 1995; Waldbusser et al. 2004; Webb and Eyre 2004). In samples with low faunal biomass, SOD was relatively low throughout the diel cycle (Figure 18), which is not unexpected in sandy sediments low in organic content (Hargrave 1972; Burdige 2006). Our measurements of SOD and the observed increase with faunal presence also agree well with chamber measurements from other studies in similar habitats. Banta et al measured basal SOD rates of 30 mmol m^{-2} d^{-1} in lab microcosms with unpopulated sandy sediments, and the addition of the polychaete *Hediste diversicolor* (formerly *Nereis diversicolor*) inflated SOD by 80-90% (Banta et al. 1999). Likewise, Webb and Eyre found that burrowing thalassinidean

shrimp in *in situ* benthic chambers increased SOD by 80% compared to unoccupied sediments (Webb and Eyre 2004).

We found significant variability in SOD on two distinct temporal scales; diel variability driven by the presence of fauna and sub-diel variability on the scale of minutes to hours. The significant interaction of DO and faunal biomass on SOD indicates that changing DO did not itself affect SOD, but rather, where fauna were present, changing DO drove shifts in their activity and behavior that affected SOD. This is consistent with our hypothesized response (H_{2B}), as well as the observations of Wenzhofer and Glud (2004), who found that the majority of nightly DO uptake could be attributed to faunal effects. However, their SOD appeared to be driven by light availability, whereas our measurements, made in shaded chambers, directly link change in SOD to DO variability. We hypothesized that fauna may flatten the relationship between DO and SOD (H_{2B}), however in the regression of the DO vs SOD slopes against faunal biomass (Figure 20A) increasing sediment faunal presence essentially inverted the relationship of DO and SOD throughout the diel cycle, surpassing even our hypothesized response. The regression of faunal biomass and the slope of DO and SOD crosses zero which indicates that there exists some tipping point where increasing faunal presence begins to drive higher nightly SOD. Our data demonstrate that the presence of fauna changes SOD patterns considerably throughout the diel cycle, and in ways that could not be predicted from measurements at any single time point or even from daytime measurements alone.

The increase in SOD in higher-populated sediments at night is presumably driven by fauna responding to low DO by increasing bioirrigation. Nereid worms irrigate their burrows (Wells and Dales 1951), and several common species are known to shift from

oxygen conforming to regulatory behaviors at low DO concentrations (Kristensen 1983). However, the two samples with highest nightly SOD values (Samples 3 and 4, Figure 17) were dominated by Orbiniids and had relatively little nereid biomass. Orbiniids are discretely motile and are not known to construct and irrigate burrows (Jumars et al. 2015) so they are unlikely to be the source of the SOD spike. More likely, these samples contained individuals of the tube-dwelling Onuphid polychaete *Diopatra cuprea* that evaded collection by retreating deep in their tubes when the sediment cores were extracted. *D. cuprea* tubes create subsurface habitat and refuge for other burrowing animals (Woodin 1978), and their irrigation activity is well documented (Mangum et al. 1968; Dales et al. 1970). Both the higher faunal abundance and the greater SOD measured in those samples may have been due to the presence of *D. cuprea*.

The short time scale of irrigation activity also explains the sub-diel variability in our measurements (Figure 18). In most of our samples, SOD varied substantially measurement-to-measurement, and samples with greater faunal presence exhibited greater high-frequency variability (Figure 22). Infauna typically irrigate intermittently in cycles of activity and rest which vary in intensity, rate and duration and be altered by DO availability (Wells and Dales 1951; Mangum et al. 1968; Kristensen 1983, 1989, 2001; Volkenborn et al. 2010, 2012; Camillini et al. 2019a). The irrigation pattern depends on the taxon, however most irrigating infauna cycle through behaviors on a scale of minutes or tens of minutes. On the time scale of our SOD incubations (~20 min) fauna intermittently irrigating likely contributed to the measurement-to-measurement variability. In sediments with large and complex faunal communities, intermittent irrigation would drive swings in SOD on very short timescales and depending on the

resident fauna. Even accounting for diel variation by measuring SOD at maximum and minimum DO and interpolating measurements between them would not accurately describe SOD dynamics throughout the entire cycle and would still yield unreliable estimates of net SOD over time.

It is common practice in sediment research to extrapolate single SOD measurements through time and space. SOD measurements taken in laboratory core incubations and with "batch" style benthic chambers are questionable in their representativeness, and the faunal effects that can substantially increase both the magnitude and the variability in SOD add important context to high-frequency eddy correlation SOD measurements. Measurement of SOD on small temporal and spatial scales has only recently become methodologically feasible but is proving potentially highly significant, and variability can now be captured but has yet to be fully explained. Our observed high spatial and temporal SOD variability, and their apparent interdependence, indicate that increasing resolution of SOD measurement in both dimensions may be not only beneficial but necessary to accurately characterize metabolic processes in these systems.

CHAPTER V OVERALL SUMMARY AND CONCLUSIONS

The objective of this dissertation research was to assess how shifts in macrofaunal activities and behavior throughout a diel oxygen cycle affect sediment metabolism rates. Shallow coastal sediments are sites of intense respiration and organic matter breakdown. Macroinfauna bioturbate and bioirrigate sediments which supplies microbes with oxygen and newly deposited organic material from surface sediments, facilitating microbial remineralization of organic matter. These processes depend heavily on the concentration of dissolved oxygen in overlying water. Shallow water oxygen patterns often follow a diel cycle as dissolved oxygen drops to hypoxic levels at night due to respiration and then increases during the day with photosynthesis, creating recurring suboxic conditions that are potentially stressful to organisms. Sediment oxygen flux is known to depend on ambient dissolved oxygen concentration, but behavioral responses of organisms to low oxygen can be complex and diverse, introducing variability into sediment metabolism rates. Additionally, the ability of sediment communities to endure and recover from brief low oxygen events may be tied to the diversity of macrofaunal bioturbation and bioirrigation methods.

In this dissertation research I examined the effects of diel changes in dissolved oxygen on macrofaunal behavior and activities and corresponding changes in sediment metabolism throughout the diel cycle. I hypothesized three possible patterns of macrofaunal response to diel oxygen variation; (1) a proportional response wherein macrofaunal activity directly co-varies with oxygen concentration, (2) a "lag" response wherein macrofauna exhibit delayed recovery from the nightly low-oxygen period, decreasing net metabolism, and (3) a "gasp" response, wherein macrofauna greatly increase their activity after the nightly low-oxygen period to recover, increasing net metabolism. To test these hypotheses, I built a

simple laboratory system to manipulate dissolved oxygen concentrations into a diel pattern. Using this system, I exposed sediment infauna to a diel oxygen cycle, observing changes in their feeding, burrowing and irrigating behaviors and measuring sediment oxygen consumption. Sediment mixing in all three of the tested taxa decreased overall throughout the experiment and over two diel cycles, but also varied proportionally with oxygen within each diel exposure. Behaviors did not show significant variation with the diel cycle, though this is likely because behaviors relevant to sediment mixing activity were not easily detected or quantified with the employed methods. These results indicate that experiments quantifying sediment mixing by macrofauna that occur in fully oxygenated conditions may not be representative of in situ rates, and that it may require more even than a single diel cycle for representative rates to emerge.

Macrofauna in natural sediments exist in communities with a diversity of behavior and activity patterns. To better understand how natural macrofaunal assemblages respond to diel cycling oxygen, I conducted a field sediment metabolism experiment. I hypothesized that in natural sediment communities, the presence of macrofaunal taxa with certain functional traits would disproportionately affect response of sediment metabolism to diel oxygen cycling. To test this hypothesis, I constructed and deployed flow-through sediment metabolism chambers to measure sediment oxygen consumption at high temporal resolution throughout a diel cycle *in situ*, and then characterized the resident macrofaunal community. We found significant variability in SOD on two distinct temporal scales; diel variability driven by the presence of fauna and sub-diel variability on the scale of minutes to hours. Our results showed that fauna change sediment metabolism patterns in ways that couldn't be predicted by single or even daytime measurements alone, and the higher

sub-diel variability, likely driven by faunal irrigation, introduces further variation that would be unaccounted for in less frequent measurements. The daily variation in SOD, and its dependence on the resident fauna, highlights the importance of capturing SOD at both high temporal and spatial resolutions.

Sediment bioturbation and metabolism, key ecosystem functions, are controlled by complex networks of interactions and feedbacks between biogeochemical and ecological processes. This research sheds new light on the connection between oxygen concentration and sediment function in these dynamic, productive marine systems and improves our understanding of the role of macrofauna in modulating that relationship.

REFERENCES

Aller, R. C. 1978. The effects of animal-sediment interactions on geochemical processes near the sediment-water interface, p. 157–172. *In* Estuarine interactions. Elsevier.

Aller, R. C. 1988. Benthic fauna and biogeochemical processes in marine sediments: the role of burrow structures. Nitrogen Cycl. Coast. Mar. Environ. 301–338.

Banta, G. T., M. Holmer, M. H. Jensen, and E. Kristensen. 1999. Effects of two polychaete worms, Nereis diversicolor and Arenicola marina, on aerobic and anaerobic decomposition in a sandy marine sediment. Aquat. Microb. Ecol. **19**: 189–204.

Berg, P., M. L. Delgard, P. Polsenaere, K. J. McGlathery, S. C. Doney, and A. C. Berger. 2019. Dynamics of benthic metabolism, O2, and pCO2 in a temperate seagrass meadow. Limnol. Oceanogr.

Berg, P., and M. Huettel. 2008. Monitoring the seafloor using the noninvasive eddy correlation technique. Oceanography **21**: 164–167.

Berg, P., M. H. Long, M. Huettel, and others. 2013. Eddy correlation measurements of oxygen fluxes in permeable sediments exposed to varying current flow and light. Limnol. Oceanogr. **58**: 1329–1343. doi:10.4319/lo.2013.58.4.1329

Berg, P., H. Roy, F. Janssen, V. Meyer, B. B. Jorgensen, M. Huettel, and D. de Beer. 2003. Oxygen uptake by aquatic sediments measured with a novel non-invasive eddy-correlation technique. Mar Ecol Prog Ser 75–83.

Bevan, D. J., and D. L. Kramer. 1988. A control system for the long-term maintenance of hypoxic water. Aquaculture **71**: 165–169.

Burdige, D. J. 2006. Geochemistry of Marine Sediments, Princeton University Press.

Burnett, L. E. 1997. The challenges of living in hypoxic and hypercapnic aquatic environments. Am. Zool. **37**: 633–640.

Calder-Potts, R., J. I. Spicer, P. Calosi, H. S. Findlay, and S. Widdicombe. 2015. A mesocosm study investigating the effects of hypoxia and population density on respiration and reproductive biology in the brittlestar Amphiura filiformis. Mar. Ecol. Prog. Ser. **534**: 135–147.

Camillini, N., M. Larsen, and R. Glud. 2019a. Behavioural patterns of the soft-shell clam Mya arenaria: implications for benthic oxygen and nitrogen dynamics. Mar. Ecol. Prog. Ser. **622**: 103–119. doi:10.3354/meps13004

Camillini, N., M. Larsen, and R. N. Glud. 2019b. Behavioural patterns of the soft-shell clam Mya arenaria: implications for benthic oxygen and nitrogen dynamics. Mar. Ecol. Prog. Ser. **622**: 103–119.

Clarke, K. R., and R. N. Gorley. 2015. PRIMER v5, v6 & v7: User manual/tutorial. Primer-E Plymouth UK **91**: 192–296.

Clavier, J., L. Chauvaud, P. Cuet, C. Esbelin, P. Frouin, D. Taddei, and G. Thouzeau. 2008. Diel variation of benthic respiration in a coral reef sediment (Reunion Island, Indian Ocean). Estuar. Coast. Shelf Sci. **76**: 369–377.

Dales, R. P. 1957. The feeding mechanism and structure of the gut of *Owenia fusiformis* delle Chiaje. J. Mar. Biol. Assoc. U. K. **36**: 81–89. doi:10.1017/S0025315400017082

Dales, R. P. 1958. Survival of Anaerobic Periods By Two Intertidal Polychaetes, *Arenicola Marina* (L.) and *Owenia Fusiformis* Delle Chiaje. J. Mar. Biol. Assoc. U. K. **37**: 521–529. doi:10.1017/S0025315400023845

Dales, R. P., C. P. Mangum, and J. C. Tichy. 1970. Effects of changes in oxygen and carbon dioxide concentrations on ventilation rhythms in onuphid polychaetes. J. Mar. Biol. Assoc. U. K. **50**: 365–380.

Diaz, R. J. 2001. Overview of hypoxia around the world. J. Environ. Qual. **30**: 275–281.

Diaz, R. J., and R. Rosenberg. 1995. Marine benthic hypoxia: a review of its ecological effects and the behavioural responses of benthic macrofauna. Oceanogr. Mar. Biol. Annu. Rev. **33**: 245–303.

Diaz, R. J., and R. Rosenberg. 2011. Introduction to environmental and economic consequences of hypoxia. Int. J. Water Resour. Dev. **27**: 71–82.

Dorgan, K. M., R. Parker, W. Ballentine, and others. 2020. Investigating the sublethal effects of oil exposure on infaunal behavior, bioturbation, and sediment oxygen consumption. Mar. Ecol. Prog. Ser. **635**: 9–24. doi:10.3354/meps13215

Eckman, J., A. Nowell, and P. Jumars. 1981. Sediment Destabilization by Animal Tubes. J. Mar. Res. **39**.

Foster, S. Q., and R. W. Fulweiler. 2019. Estuarine Sediments Exhibit Dynamic and Variable Biogeochemical Responses to Hypoxia. J. Geophys. Res. Biogeosciences **124**: 737–758.

Friard, O., and M. Gamba. 2016. BORIS: a free, versatile open-source event-logging software for video/audio coding and live observations. Methods Ecol. Evol. **7**: 1325–1330. doi:10.1111/2041-210X.12584

Froelich, P., G. P. Klinkhammer, M. L. Bender, and others. 1979. Early oxidation of organic matter in pelagic sediments of the eastern equatorial Atlantic: suboxic diagenesis. Geochim. Cosmochim. Acta **43**: 1075–1090.

Gadeken, K. J., and K. M. Dorgan. 2021. A Simple and Inexpensive Method for Manipulating Dissolved Oxygen in the Lab. Oceanography **34**: 177–183.

Gammal, J., J. Norkko, C. A. Pilditch, and A. Norkko. 2017. Coastal hypoxia and the importance of benthic macrofauna communities for ecosystem functioning. Estuaries Coasts **40**: 457–468.

Gobler, C. J., E. L. DePasquale, A. W. Griffith, and H. Baumann. 2014. Hypoxia and acidification have additive and synergistic negative effects on the growth, survival, and metamorphosis of early life stage bivalves. PloS One **9**: e83648.

Grecay, P. A., and K. L. Stierhoff. 2002. A device for simultaneously controlling multiple treatment levels of dissolved oxygen in laboratory experiments. J. Exp. Mar. Biol. Ecol. **280**: 53–62.

Gurr, S. J., J. Goleski, F. P. Lima, R. Seabra, C. J. Gobler, and N. Volkenborn. 2018. Cardiac responses of the bay scallop Argopecten irradians to diel-cycling hypoxia. J. Exp. Mar. Biol. Ecol. **500**: 18–29.

Hargrave, B. T. 1972. Aerobic Decomposition of Sediment and Detritus as a Function of Particle Surface Area and Organic Content. Limnol. Oceanogr. **17**: 583–586. doi:10.4319/lo.1972.17.4.0583

Herreid II, C. F. 1980. Hypoxia in invertebrates. Comp. Biochem. Physiol. A Physiol. **67**: 311–320.

Huettel, M., P. Berg, and J. E. Kostka. 2014. Benthic Exchange and Biogeochemical Cycling in Permeable Sediments. Annu. Rev. Mar. Sci. **6**: 23–51. doi:10.1146/annurev-marine-051413-012706

Jackson, D., and M. Richardson. 2007. High-frequency seafloor acoustics, Springer Science & Business Media.

Jumars, P. A., K. M. Dorgan, and S. M. Lindsay. 2015. Diet of Worms emended: An Update of Polychaete Feeding Guilds Appendix A Family-by-Family Updates. Annu. Rev. Mar. Sci. **7**: 497–520.

Kristensen, E. 1983. Ventilation and oxygen uptake by three species of Nereis (Annelida: Polychaeta). I. Effects of hypoxia. Mar Ecol Prog Ser **12**: 289–297.

Kristensen, E. 1989. Oxygen and carbon dioxide exchange in the polychaete Nereis virens: influence of ventilation activity and starvation. Mar. Biol. **101**: 381–388. doi:10.1007/BF00428134

Kristensen, E. 2001. Impact of polychaetes (Nereis spp. and Arenicola marina) on carbon biogeochemistry in coastal marine sediments. Geochem. Trans. **2**: 92.

Lehrter, J. C., D. L. Beddick, R. Devereux, D. F. Yates, and M. C. Murrell. 2012. Sediment-water fluxes of dissolved inorganic carbon, O 2, nutrients, and N 2 from the hypoxic region of the Louisiana continental shelf. Biogeochemistry **109**: 233–252.

Levin, L. A., W. Ekau, A. J. Gooday, and others. 2009. Effects of natural and human-induced hypoxia on coastal benthos. Biogeosciences 2063–2098.

Long, W. C., B. J. Brylawski, and R. D. Seitz. 2008. Behavioral effects of low dissolved oxygen on the bivalve Macoma balthica. J. Exp. Mar. Biol. Ecol. **359**: 34–39.

Mangum, C. P., S. L. Santos, and W. R. Rhodes. 1968. Distribution and feeding in the onuphid polychaete, Diopatra cuprea (Bosc). Mar. Biol. **2**: 33–40.

Mangum, C., and W. V. Winkle. 1973. Responses of Aquatic Invertebrates to Declining Oxygen Conditions. Am. Zool. **13**: 529–541. doi:10.1093/icb/13.2.529

McCarthy, M. J., K. S. McNeal, J. W. Morse, and W. S. Gardner. 2008. Bottom-water hypoxia effects on sediment–water interface nitrogen transformations in a seasonally hypoxic, shallow bay (Corpus Christi Bay, TX, USA). Estuaries Coasts **31**: 521–531.

Mermillod-Blondin, F., and R. Rosenberg. 2006. Ecosystem engineering: the impact of bioturbation on biogeochemical processes in marine and freshwater benthic habitats. Aquat. Sci. **68**: 434–442.

Mermillod-Blondin, F., R. Rosenberg, F. François-Carcaillet, K. Norling, and L. Mauclaire. 2004. Influence of bioturbation by three benthic infaunal species on microbial communities and biogeochemical processes in marine sediment. Aquat. Microb. Ecol. **36**: 271–284.

Meysman, F. J., J. J. Middelburg, and C. H. Heip. 2006. Bioturbation: a fresh look at Darwin's last idea. Trends Ecol. Evol. **21**: 688–695.

Michaud, E., G. Desrosiers, F. Mermillod-Blondin, B. Sundby, and G. Stora. 2005. The functional group approach to bioturbation: the effects of biodiffusers and gallery-diffusers of the Macoma balthica community on sediment oxygen uptake. J. Exp. Mar. Biol. Ecol. **326**: 77–88.

Middelburg, J. J., and L. A. Levin. 2009. Coastal hypoxia and sediment biogeochemistry. Biogeosciences **6**: 1273–1293.

Miller, D. C., D. E. Body, J. C. Sinnett, S. L. Poucher, J. Sewall, and D. J. Sleczkowski. 1994. A reduced dissolved oxygen test system for marine organisms. Aquaculture **123**: 167–171.

Modig, H., and E. Ólafsson. 1998. Responses of Baltic benthic invertebrates to hypoxic events. J. Exp. Mar. Biol. Ecol. **229**: 133–148.

Mount, D. I. 1961. Development of a System for Controlling Dissolved-Oxygen Content of Water. Trans. Am. Fish. Soc. **90**: 323–327.

Neubacher, E. C., R. E. Parker, and M. Trimmer. 2013. The potential effect of sustained hypoxia on nitrogen cycling in sediment from the southern North Sea: a mesocosm experiment. Biogeochemistry **113**: 69–84.

Nilsson, H. C., and R. Rosenberg. 1994. Hypoxic response of two marine benthic communities. Mar. Ecol. Prog. Ser. Oldendorf **115**: 209–217.

Nilsson, H. C., and M. Skold. 1996. Arm regeneration and spawning in the brittle star Amphiura Jiliformis (O.F. Miiller) during hypoxia. J. Exp. Mar. Biol. Ecol. **199**: 193–206.

Noffke, A., G. Hertweck, I. Kröncke, and A. Wehrmann. 2009. Particle size selection and tube structure of the polychaete Owenia fusiformis. Estuar. Coast. Shelf Sci. **81**: 160–168. doi:10.1016/j.ecss.2008.10.010

Norling, K., R. Rosenberg, S. Hulth, A. Grémare, and E. Bonsdorff. 2007. Importance of functional biodiversity and species-specific traits of benthic fauna for ecosystem functions in marine sediment. Mar. Ecol. Prog. Ser. **332**: 11–23.

Pelegri, S. P., and T. H. Blackburn. 1995. Effect of bioturbation by Nereis sp., Mya arenaria and Cerastoderma sp. on nitrification and denitrification in estuarine sediments. Ophelia **42**: 289–299.

Peterson, M. S., and B. E. Ardahl. 1992. Automated maintenance of dissolved oxygen concentrations in flow-through aquaria. Aquaculture **101**: 379–384.

Prosser, C. L. 1973. Oxygen: respiration and metabolism, p. 165–211. *In* Comparative Animal Physiology. W. B. Saunders Company.

Rasband, W. 2018. ImageJ, US National Institutes of Health, Bethesda, MD.

Riedel, B., T. Pados, K. Pretterebner, L. Schiemer, A. Steckbauer, A. Haselmair, M. Zuschin, and M. Stachowitsch. 2014. Effect of hypoxia and anoxia on invertebrate behaviour: ecological perspectives from species to community level. Biogeosciences **11**: 1491–1518.

Rosenberg, R., B. Hellman, and B. Johansson. 1991. Hypoxic tolerance of marine benthic fauna. Mar. Ecol. Prog. Ser. Oldendorf **79**: 127–131.

Rosenberg, R., and L. Lundberg. 2004. Photoperiodic activity pattern in the brittle star Amphiura filiformis. Mar. Biol. **145**: 651–656.

Rosenberg, R., H. C. Nilsson, and R. J. Diaz. 2001. Response of benthic fauna and changing sediment redox profiles over a hypoxic gradient. Estuar. Coast. Shelf Sci. **53**: 343–350.

Seitz, R. D., D. M. Dauer, R. J. Llansó, and W. C. Long. 2009. Broad-scale effects of hypoxia on benthic community structure in Chesapeake Bay, USA. J. Exp. Mar. Biol. Ecol. **381**: S4–S12.

Seitz, R. D., L. S. Marshall Jr, A. H. Hines, and K. L. Clark. 2003. Effects of hypoxia on predator-prey dynamics of the blue crab Callinectes sapidus and the Baltic clam Macoma balthica in Chesapeake Bay. Mar. Ecol. Prog. Ser. **257**: 179–188.

Solan, M., B. D. Wigham, I. R. Hudson, R. Kennedy, C. H. Coulon, K. Norling, H. C. Nilsson, and R. Rosenberg. 2004. In situ quantification of bioturbation using time lapse fluorescent sediment profile imaging (f SPI), luminophore tracers and model simulation. Mar. Ecol. Prog. Ser. **271**: 1–12.

Sturdivant, S. K., R. J. Díaz, and G. R. Cutter. 2012. Bioturbation in a declining oxygen environment, in situ observations from Wormcam. PloS One **7**: e34539.

Tengberg, A., F. De Bovee, P. Hall, and others. 1995. Benthic chamber and profiling landers in oceanography — A review of design, technical solutions and functioning. Prog. Oceanogr. **35**: 253–294. doi:10.1016/0079-6611(95)00009-6

The MathWorks Inc. 2021. MATLAB,.

Thetmeyer, H., U. Waller, K. D. Black, S. Inselmann, and H. Rosenthal. 1999. Growth of European sea bass (Dicentrarchus labrax L.) under hypoxic and oscillating oxygen conditions. Aquaculture **174**: 355–367.

Tyler, R. M., D. C. Brady, and T. E. Targett. 2009. Temporal and spatial dynamics of diel-cycling hypoxia in estuarine tributaries. Estuaries Coasts **32**: 123–145.

Vismann, B. 1990. Sulfide detoxification and tolerance in Nereis(Hediste) diversicolor and Nereis(Neanthes) virens(Annelida: Polychaeta). Mar. Ecol. Prog. Ser. Oldendorf **59**: 229–238.

Vistisen, B., and B. Vismann. 1997. Tolerance to low oxygen and sulfide in Amphiura filiformis and Ophiura albida (Echinodermata: Ophiuroidea). Mar. Biol. **128**: 241–246. doi:10.1007/s002270050088

Volkenborn, N., C. Meile, L. Polerecky, and others. 2012. Intermittent bioirrigation and oxygen dynamics in permeable sediments: An experimental and modeling study of three tellinid bivalves. J. Mar. Res. **70**: 794–823.

Volkenborn, N., L. Polerecky, D. S. Wethey, and S. A. Woodin. 2010. Oscillatory porewater bioadvection in marine sediments induced by hydraulic activities of Arenicola marina. Limnol. Oceanogr. **55**: 1231–1247.

Vopel, K., D. Thistle, and R. Rosenberg. 2003. Effect of the brittle star Amphiura filiformis (Amphiuridae, Echinodermata) on oxygen flux into the sediment. Limnol. Oceanogr. **48**: 2034–2045. doi:10.4319/lo.2003.48.5.2034

Waldbusser, G. G., R. L. Marinelli, R. B. Whitlatch, and P. T. Visscher. 2004. The effects of infaunal biodiversity on biogeochemistry of coastal marine sediments. Limnol. Oceanogr. **49**: 1482–1492.

Webb, A., and B. Eyre. 2004. Effect of natural populations of burrowing thalassinidean shrimp on sediment irrigation, benthic metabolism, nutrient fluxes and denitrification. Mar. Ecol. Prog. Ser. **268**: 205–220. doi:10.3354/meps268205

Weissberger, E. J., L. L. Coiro, and E. W. Davey. 2009. Effects of hypoxia on animal burrow construction and consequent effects on sediment redox profiles. J. Exp. Mar. Biol. Ecol. **371**: 60–67.

Wells, G. P., and R. P. Dales. 1951. Spontaneous activity patterns in animal behaviour: the irrigation of the burrow in the polychaetes Chaetopterus variopedatus Renier and Nereis diversicolor OF Müller. J. Mar. Biol. Assoc. U. K. **29**: 661–680.

Wenner, E., D. Sanger, M. Arendt, A. F. Holland, and Y. Chen. 2004. Variability in dissolved oxygen and other water-quality variables within the national estuarine research reserve system. J. Coast. Res. 17–38.

Wenzhöfer, F., and R. N. Glud. 2004. Small-scale spatial and temporal variability in coastal benthic O2 dynamics: Effects of fauna activity. Limnol. Oceanogr. **49**: 1471–1481.

Widdicombe, S., and M. Austen. 1999. Mesocosm investigation into the effects of bioturbation on the diversity and structure of a subtidal macrobenthic community. Mar. Ecol. Prog. Ser. **189**: 181–193. doi:10.3354/meps189181

Woodin, S. A. 1978. Refuges, disturbance, and community structure: a marine soft-bottom example. Ecology **59**: 274–284.

Woodley, J. D. 1975. The behaviour of some Amphiurid brittlestars. J. Exp. Mar. Biol. Ecol. **18**: 18.

Zorn, M. E., S. V. Lalonde, M. K. Gingras, S. G. Pemberton, and K. O. Konhauser. 2006. Microscale oxygen distribution in various invertebrate burrow walls. Geobiology **4**: 137–145.

APPENDICES

Appendix A Chapter III Supporting Information

The supporting information presented here includes detailed drawings of the benthic metabolism chambers (Figure A1), a schematic wiring diagram contained in the central housing (Figure A2), and the Arduino code for the system (Text A1).

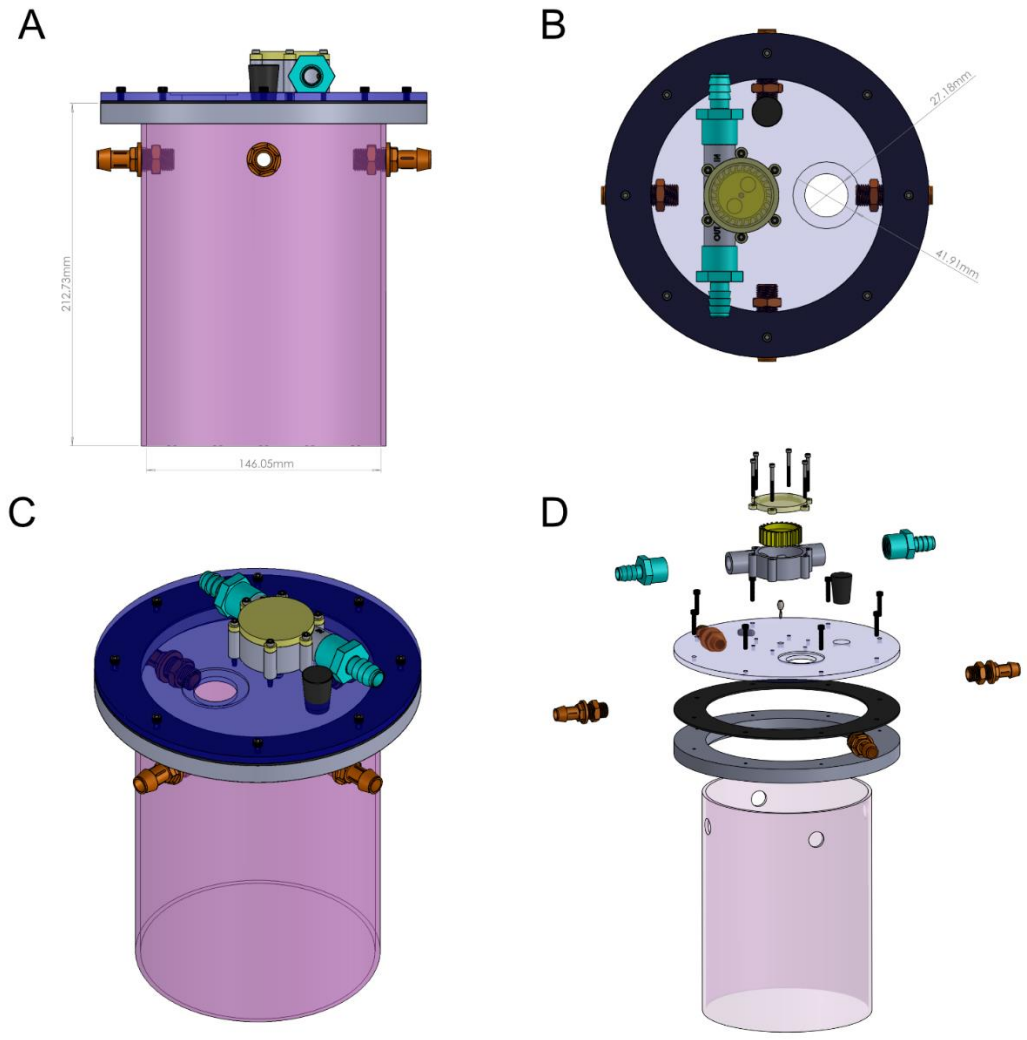

Figure A1. Detailed drawings of the chamber assembly with views from A) side, B) top, C) isometric, and D) exploded into components.

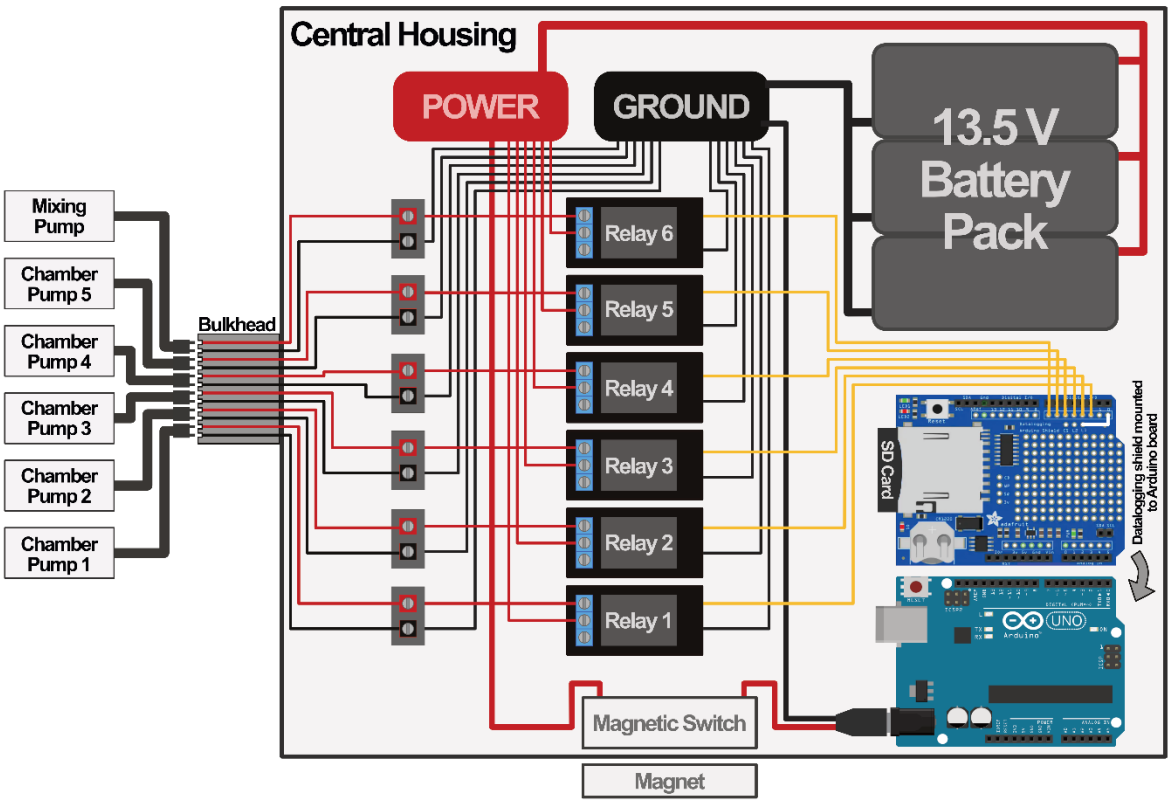

Figure A2. Electronics and wiring diagram for central housing.

Text A1: Arduino code

```
#include <SoftwareSerial.h>
#include <SPI.h>
#include <Wire.h>
#include <SD.h>
#include <RTClib.h>

const int chipSelect = 10;
File logfile;
char filename[] = "Logger00.csv";
RTC_PCF8523 rtc;

int FLOWpin = 0;
int MIXpin = 7;

//------------------------------------------------- SETUP ----------------------------------
----------
void setup() {
```

```
  Serial.begin(9600);
    while(!Serial){              //wait for serial port to connect before proceeding
   ;
   }

   rtc.begin();
   if(!rtc.begin()){                        //checking to see if rtc started...
    Serial.println("Couldn't find RTC");       //nope, didn't start, OR...
    while(1);
   }
  else if(!rtc.initialized()){
    Serial.println("RTC NOT running");       //isn't running right
  }
  else {
    Serial.println("RTC is running");
  }

 //rtc.adjust(DateTime(F(__DATE__), F(__TIME__)));

  Serial.print("Initializing SD card...");
    if(!SD.begin(chipSelect)){                    //checks that communication with SD card
is working...
      Serial.println("SD failed, or not present");      //nope, didn't work, OR...
    }
    else {
      Serial.println("SD initialized");               //worked
    }

delay(10);

  Serial.print("Creating new file...");
  for (byte i = 0; i < 100; i++) {                  //check files on the SD card, counting up
from LOGGER00, LOGGER01, etc.
    filename[6] = i/10 + '0';
    filename[7] = i%10 + '0';
    if (!SD.exists(filename)) {                     //only open a new file if one with that name
doesn't exist already
      logfile = SD.open(filename, FILE_WRITE);
      delay(10);
    break;
    }
  }

  logfile = SD.open(filename, FILE_WRITE);          //try opening newly created and
named file
```

```
  if (!logfile) {                          //logfile wouldn't open...
    Serial.println("Couldn't create file");
  }
  else {
    Serial.print("Logging to: ");              //If logfile was successfully opened, print
name of new file
    Serial.println(filename);
    String headerString = "year,month,day,hour,minute,second";    //create column
headers
    logfile.println(headerString); //add headers as first line in new file
    delay(10);
    logfile.close();
  }

for(int FLOWpin = 2; FLOWpin <= 6; FLOWpin++) {
 pinMode(FLOWpin, OUTPUT);
  }
for(int FLOWpin = 2; FLOWpin <= 6; FLOWpin++) {
 digitalWrite(FLOWpin, LOW);
  }

pinMode(MIXpin, OUTPUT);
digitalWrite(MIXpin, LOW);

}

//------------------------------------------------- LOOP ----------------------------------------
---------
void loop() {
 log_DandT();

 for(int FLOWpin = 2; FLOWpin <= 6; FLOWpin++) {    //flush step
  digitalWrite(FLOWpin, HIGH);
  delay(20000);
  digitalWrite(FLOWpin, LOW);
  }

 for(int j = 1; j <= 20; j++) {                  //mix step
  digitalWrite(MIXpin, HIGH);
  delay(20000);
  digitalWrite(MIXpin, LOW);
  delay(40000);
  }
 }
```

```
//-----------------------------------------Date and Time Logging-----------------------------
--------------
void log_DandT() {
  String dataString = "";
  DateTime now = rtc.now();
  dataString += now.year();
  dataString += ",";
  dataString += now.month();
  dataString += ",";
  dataString += now.day();
  dataString += ",";
  dataString += now.hour();
  dataString += ",";
  dataString += now.minute();
  dataString += ",";
  dataString += now.second();

    logfile = SD.open(filename, FILE_WRITE);
    if (!logfile) {
      Serial.println("Error  opening file");
    }
  logfile.println(dataString);
  logfile.close();

delay(10);

    Serial.print("(");
    Serial.print(now.year(), DEC);
    Serial.print('/');
    Serial.print(now.month(), DEC);
    Serial.print('/');
    Serial.print(now.day(), DEC);
    Serial.print(") ");
    Serial.print(now.hour(), DEC);
    Serial.print(':');
    Serial.print(now.minute(), DEC);
    Serial.print(':');
    Serial.println(now.second(), DEC);

    delay(10);
}
```

Appendix B Chapter IV Supporting Information

The supporting information presented here includes a figure demonstrating the iterative smoothing fit analysis (Figure A1), DO and temperature for each of the three field deployments (Figure A2), sediment geochemical characteristics (Figure A3), and the regressions of SOD against DO for each of the samples (Figure A4).

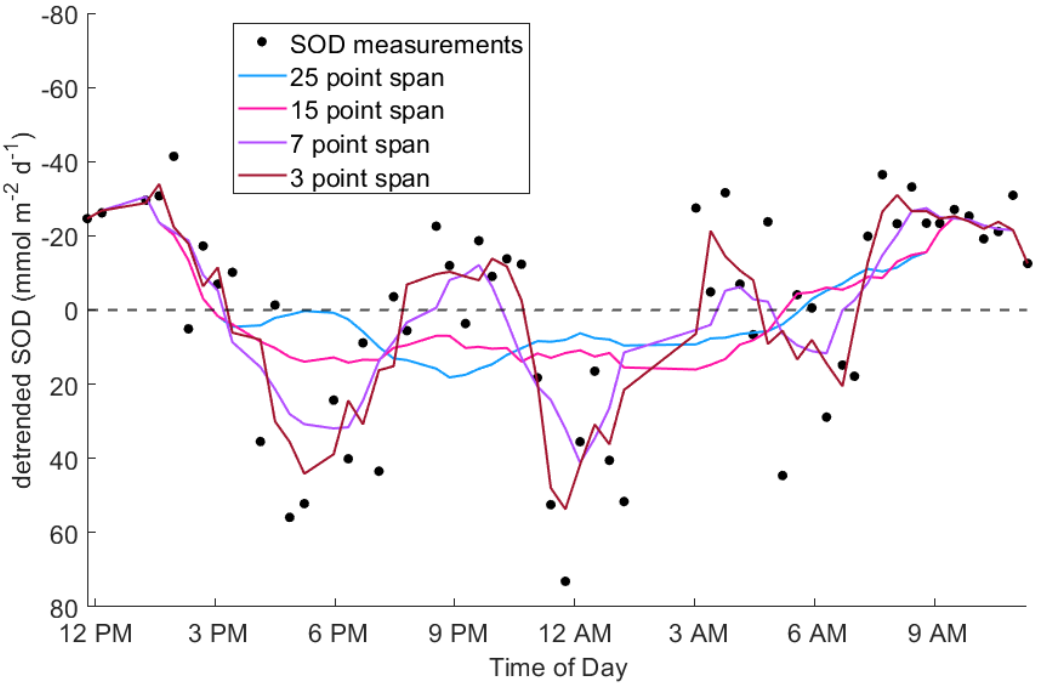

Figure B1. Example of smoothing by fitting moving averages of varying span sizes (data is from deployment 1, sample 1). Averages were only taken of an odd number of data points because points were sampled symmetrically around the calculation point.

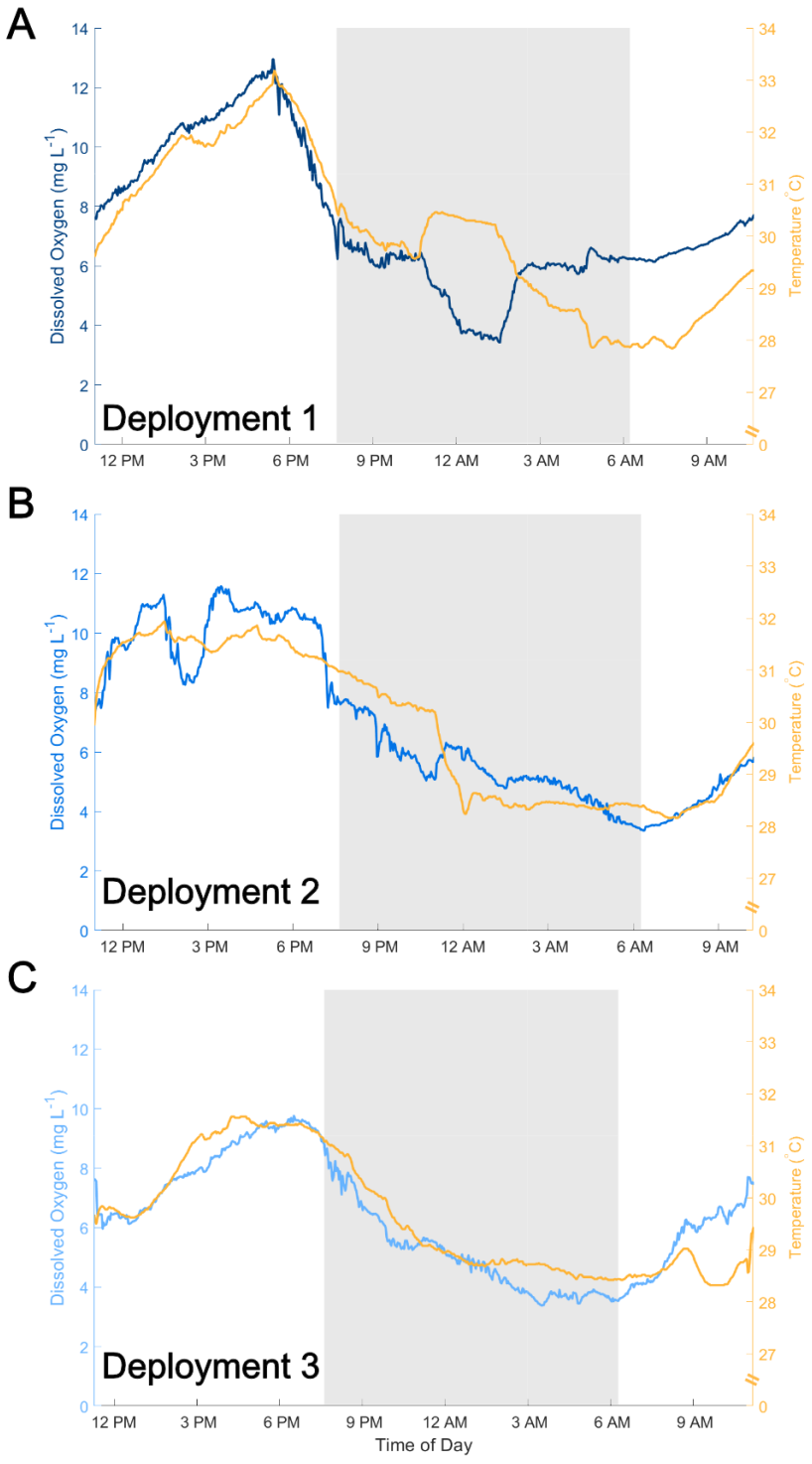

Figure B2. Ambient dissolved oxygen and temperature from HOBO logger for the three deployments (A-C).

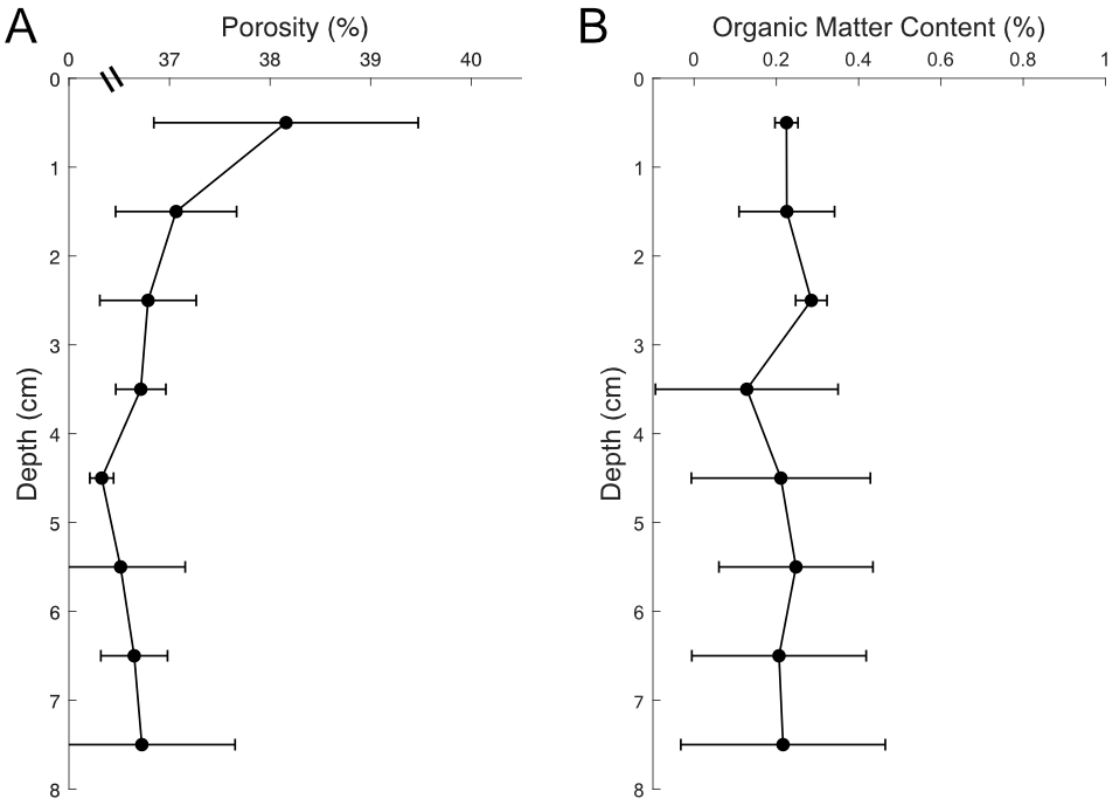

Figure B3. Sediment geochemical characteristics, (A) porosity and (B) organic matter content, as percent weight. Note the different x-axis scales.

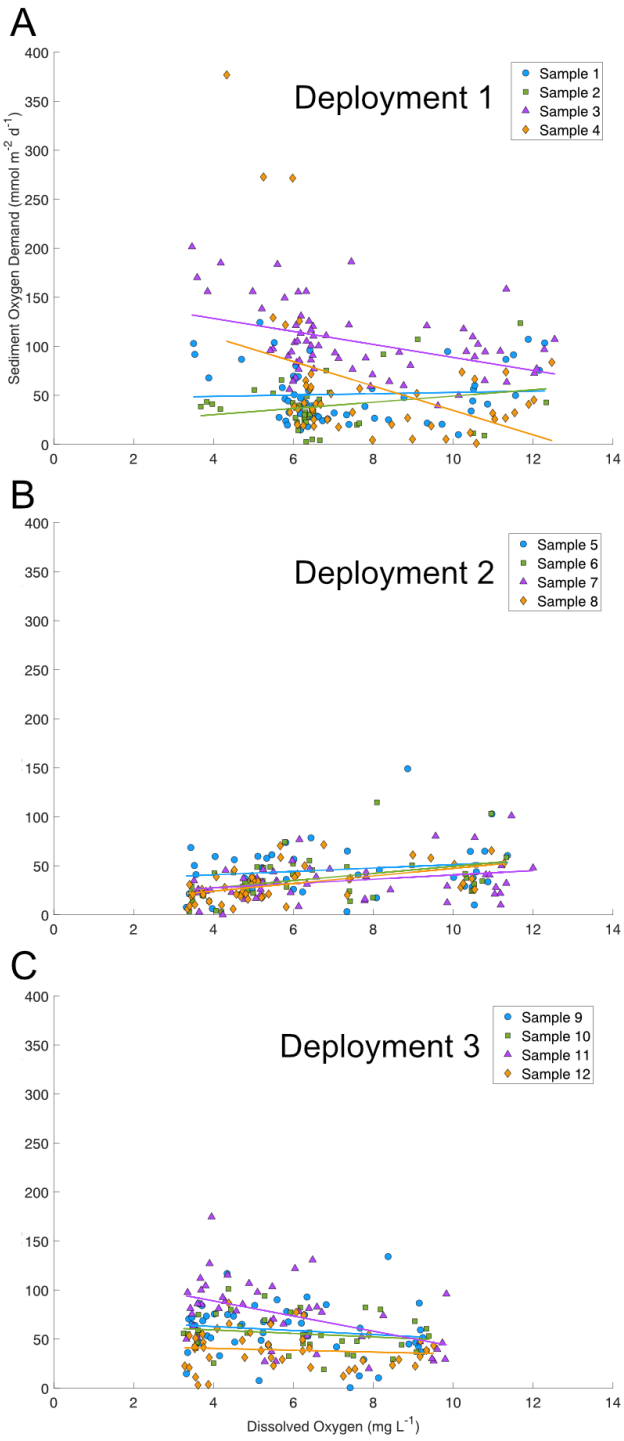

Figure B4. SOD plotted against the initial DO of the incubation for each sample in Deployments 1 (A), 2 (B) and 3 (C). Points are the individual values for each incubation, and lines are the regressions among all incubations for that sample.

BIOGRAPHICAL SKETCH

Name of Author: Kara J. Gadeken

Graduate and Undergraduate Schools Attended:

University of South Alabama, Mobile, Alabama, USA
College of William & Mary, Williamsburg, Virginia, USA

Degrees Awarded:

Doctorate of Philosophy in Marine Sciences, 2022
Bachelor of Science in Biology and Minor in Marine Science, 2014

Awards and Honors:

2021 NSF OCE Postdoctoral Research Fellowship (PRFP), Chemical Oceanography
2020 USA Dr. Robert Shipp Award for Outstanding PhD Student in Marine Sciences
University of South Alabama Marine Sciences Department Fellowship

Publications and Published Data Sets:

Gadeken, K. J., Clemo, W. C., Ballentine, W., Dykstra, S. J., Fung, M., Hagemeyer, A., Dorgan, K. M., Dzwonkowski, B. *In press.* Transport of biodeposits and benthic footprint around an oyster farm, Damariscotta Estuary, Maine. *PeerJ.*

Gadeken, K. J., Dorgan, K. M. 2021. A simple and inexpensive method to manipulate dissolved oxygen in the lab. *DIY Oceanography,* 34(2).

Dorgan, K. M., Parker, R., Ballentine, W., Berke, S.K, Kiskaddon, E., **Gadeken, K. J.,** Weldin, E., Clemo, W. C., Caffray, T., Budai, S., Bell. S. 2020. Investigating the sublethal effects of oil exposure on infaunal behavior, bioturbation, and sediment oxygen consumption. *Marine Ecology Progress Series*, 635:9-24.